HHS Public Access

Author manuscript

Cell Rep. Author manuscript; available in PMC 2019 November 20.

Published in final edited form as:

Cell Rep. 2019 November 05; 29(6): 1511–1523.e5. doi:10.1016/j.celrep.2019.09.070.

Metformin Improves Mitochondrial Respiratory Activity through Activation of AMPK

Yu Wang[1,9], **Hongying An**[2,9], **Ting Liu**[3], **Caolitao Qin**[2], **Hiromi Sesaki**[4], **Shaodong Guo**[6], **Sally Radovick**[7], **Mehboob Hussain**[8], **Akhil Maheshwari**[1], **Fredric E. Wondisford**[7], **Brian O'Rourke**[3], **Ling He**[1,2,5,10,*]

[1]Division of Neonatology, Johns Hopkins University School of Medicine, Baltimore, MD 21287, USA

[2]Division of Metabolism, Johns Hopkins University School of Medicine, Baltimore, MD 21287, USA

[3]Department of Medicine, Johns Hopkins University School of Medicine, Baltimore, MD 21287, USA

[4]Department of Cell Biology, Johns Hopkins University School of Medicine, Baltimore, MD 21287, USA

[5]Department of Pharmacology and Molecular Sciences, Johns Hopkins University School of Medicine, Baltimore, MD 21287, USA

[6]Department of Nutrition and Food Science, Texas A&M University, TX 77843, USA

[7]Departments of Pediatrics and Medicine, Rutgers-Robert Wood Johnson Medical School, New Brunswick, NJ 08901, USA

[8]Division of Metabolism, Endocrinology and Diabetes, University of Michigan Medical School, Ann Arbor, MI 48105, USA

[9]These authors contributed equally

[10]Lead Contact

SUMMARY

Impaired mitochondrial respiratory activity contributes to the development of insulin resistance in type 2 diabetes. Metformin, a first-line antidiabetic drug, functions mainly by improving patients' hyperglycemia and insulin resistance. However, its mechanism of action is still not well

*Correspondence: heling@jhmi.edu.

AUTHOR CONTRIBUTIONS

L.H. designed the experiments, managed the project, and coordinated activities from all authors. Y.W., H.A., T.L., C.Q., and L.H. conducted experiments. T.L. and B.O. guided the Seahorse assays. H.S. generated and provided Drp1 KO mice. S.G. determined metabolic parameters in the blood samples. A.M. supported the analysis of the confocal images. S.R., M.H., F.E.W., and L.H. analyzed the data and wrote the manuscript.

DECLARATION OF INTERESTS

The authors declare no competing interests

SUPPLEMENTAL INFORMATION

Supplemental Information can be found online at https://doi.org/10.1016/j.celrep.2019.09.070.

understood. We show here that pharmacological metformin concentration increases mitochondrial respiration, membrane potential, and ATP levels in hepatocytes and a clinically relevant metformin dose increases liver mitochondrial density and complex 1 activity along with improved hyperglycemia in high-fat- diet (HFD)-fed mice. Metformin, functioning through 5′ AMP-activated protein kinase (AMPK), promotes mitochondrial fission to improve mitochondrial respiration and restore the mitochondrial life cycle. Furthermore, HFD-fed-mice with liver-specific knockout of AMPKα1/2 subunits exhibit higher blood glucose levels when treated with metformin. Our results demonstrate that activation of AMPK by metformin improves mitochondrial respiration and hyperglycemia in obesity. We also found that supra-pharmacological metformin concentrations reduce adenine nucleotides, resulting in the halt of mitochondrial respiration. These findings suggest a mechanism for metformin's anti-tumor effects.

In Brief

The mechanism of metformin action still remains controversial, in particular on mitochondrial activity and the involvement of AMPK. Wang et al. show that pharmacological metformin concentration or dose improves mitochondrial respiration by increasing mitochondrial fission through AMPK-Mff signaling; in contrast, supra-pharmacological metformin concentrations reduce mitochondrial respiration through decreasing adenine nucleotide levels.

Graphical Abstract

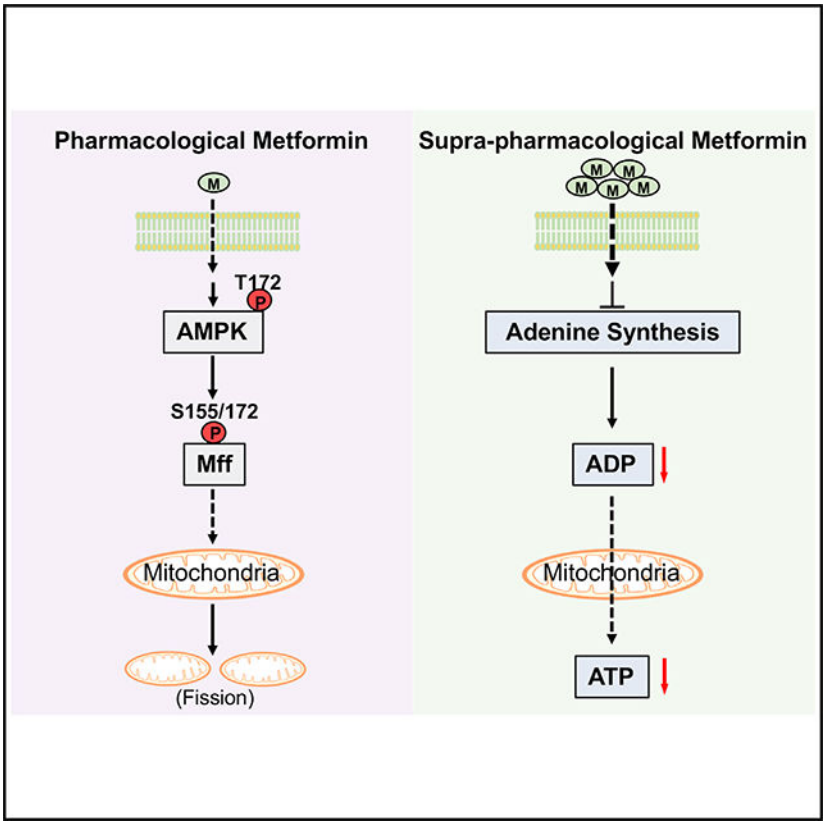

INTRODUCTION

Patients with type 2 diabetes (T2D) have decreased mitochondrial number and respiratory activity, and mitochondrial dysfunction is implicated in the development of T2D (Cheng et al., 2009, 2010; Morino et al., 2005; Petersen et al., 2004; Ritov et al., 2005). As the primary organelles responsible for nutrient metabolism and oxidative phosphorylation, mitochondria continually undertake fusion and fission processes for maintenance of a healthy mitochondrial population and regulation of bioenergetic efficiency and energy expenditure (Liesa and Shirihai, 2013; Youle and van der Bliek, 2012). Abnormal mitochondrial life cycle, such as inhibition of mitochondrial fission, leads to decreased mitochondrial respiration and functions (Twig et al., 2008; Yamada et al., 2018). This line of evidence suggests that mitochondrial fission is associated with increased mitochondrial respiratory capacity and nutrient oxidation.

Metformin is now the most widely prescribed oral anti-diabetic agent worldwide, taken by over 150 million people annually (He and Wondisford, 2015). Metformin improves hyperglycemia in T2D mainly through suppression of liver glucose production and alleviation of insulin resistance (Hundal et al., 2000; Takashima et al., 2010). However, its mechanism of action remains only partially understood and controversial. In particular, whether metformin functions through the inhibition of mitochondrial respiratory chain activity or the activation of 5′ AMP-activated protein kinase (AMPK). Metformin was reported to activate AMPK (Hawley et al., 2002; Zhou et al., 2001). AMPK is a heterotrimeric complex consisting of an α catalytic subunit, scaffold protein β subunit, and regulatory γ non-catalytic subunit (Hardie et al., 2012). Metformin activates AMPK by increasing the phosphorylation of the catalytic α subunit at T172 (Hawley et al., 2002; Zhou et al., 2001), and metformin fails to improve hyperglycemia in mice with liver-specific knockout of LKB1, the upstream kinase for AMPKα subunit phosphorylation at T172 (Shaw et al., 2005). We reported that metformin activates AMPK by promoting the formation of the functional AMPKαβγ heterotrimeric complex and phosphorylation of the CREB-binding protein (He et al., 2009, 2014; Meng et al., 2015). Metformin can inhibit mitochondrial glycerol 3-phosphate dehydrogenase, leading to the suppression of gluconeogenesis by preventing the use of lactate (Madiraju et al., 2014). This metformin effect could be involved in the AMPK because mitochondrial glycerol 3-phosphate dehydrogenase is negatively regulated by AMPK (Lee et al., 2012). Mice with mutations of AMPK-targeted phosphorylation sites in acetyl-coenzyme A (CoA) carboxylase 1 and 2 exhibited insulin resistance (Fullerton et al., 2013). These studies support a mechanism for metformin action through activation of the LKB1-AMPK pathway.

It has also been proposed that the principal mechanism of metformin action is through an AMPK-independent pathway (Foretz et al., 2010; Miller et al., 2013). Previous reports have shown that metformin can reduce cellular oxygen consumption by inhibiting mitochondrial complex 1 activity (El-Mir et al., 2000; Owen et al., 2000), and yet, inhibition of cellular respiration requires high concentrations of metformin (~5 mM) (El-Mir et al., 2000; Owen et al., 2000). Of note, to achieve the high metformin concentrations in mitochondria, digitonin-permeabilized hepatocytes were used in these studies (El-Mir et al., 2000; Owen et al., 2000). These supra-metformin concentrations have been used to prevent tumor growth (Lee

et al., 2019). Defects in mitochondrial respiratory chain activity were reported to contribute to the development of insulin resistance and hyperglycemia in T2D (Kelley et al., 2002; Morino et al., 2005; Petersen et al., 2004; Ritov et al., 2005). If metformin indeed functions by inhibiting mitochondrial complex 1 activity, this should further aggravate insulin resistance and hyperglycemia in diabetic patients, against metformin's therapeutic effects in T2D. In addition, human studies showed that metformin is able to activate mitochondrial respiratory chain activity (Larsen et al., 2012; Victor et al., 2015). These paradoxical effects of metformin published in the literature promote us to investigate whether clinically relevant doses and pharmacological concentrations of metformin could affect mitochondrial respiratory chain activity in the liver and primary hepatocytes and the involvement of AMPK.

RESULTS

Supra-pharmacological Metformin Concentrations Result in Reduction of Adenine Nucleotides and Mitochondrial Respiration

In agreement with previous studies that supra-pharmacological concentrations of metformin can reduce the oxygen consumption rate (El-Mir et al., 2000; Owen et al., 2000), we found that supra-pharmacological metformin concentrations (500 and 1,000 μM) significantly decreased basal respiration, ATP-linked respiration, maximal respiration capacity, and non-mitochondrial respiration in primary hepatocytes treated with serial concentrations of metformin (Figures 1A and 1B). Treatment with supra-pharmacological metformin concentrations drastically reduced cellular AMP, ADP, and ATP levels (Figures 1C and 1D) and elevated AMP/ATP ratios (Figure 1E). Having seen the drastic reduction of total adenine nucleotides in primary hepatocytes treated with supra-pharmacological metformin concentrations, we determined the mRNA levels of genes related to the metabolism of adenine nucleotides. Treatment with 1,000 μM of metformin reduced *adenylosuccinate synthetase* (*AdSS*) and *adenylosuccinate lyase* (*AdSL*) mRNA levels by ~60% without a significant change in the genes correlated to the conversion and salvation of adenine nucleotides (Figure 1F), suggesting that supra-pharmacological concentrations of metformin decrease adenine nucleotides mainly through the suppression of adenine synthesis. Treatment with 1,000 μM of metformin led to a mild reduction in the mRNA levels of *5′-nucleotidase* (*Nt5e*) and *adenosine deaminase* (*Ada*) genes that related to the degradation of adenine nucleotides, which may be due to a compensatory response to the drastic decrease in adenine nucleotides.

A previous report showed treatment with supra-pharmacological metformin concentrations (1,000 μM) did not reduce the mitochondrial membrane potential (Wheaton et al., 2014), and we found that treatment with supra-pharmacological metformin concentrations (500 and 1,000 μM) did not reduce the mitochondrial membrane potential in primary hepatocytes (Figure 1G). On the contrary, treatment with 1,000 μM of metformin significantly increased the mitochondrial membrane potential in Hepa 1–6 (hepatocyte-derived), C2C12 (muscle-derived), and Hek293 (kidney-derived) (Figure 1H). Supra-pharmacological metformin concentrations drastically reduced ADP levels (Figure 1C), and inhibition of ATP synthesis by oligomycin reduced ATP levels but increased mitochondrial membrane potential (Lee and

Yoon, 2014). As such, we tested whether the reduction of oxygen consumption by a supra-pharmacological metformin concentration is due to insufficient levels of cellular ADP, which would lead to an inability to utilize the mitochondrial membrane potential to generate ATP. To test this notion, two concentrations (0.5 and 2.5 mM) of ADP were supplemented in the assay buffer during the determination of oxygen consumption rate. The addition of ADP had no effect on oxygen consumption rate in primary hepatocytes without metformin treatment (Figure 1I). In contrast, the addition of ADP significantly increased the oxygen consumption rate in primary hepatocytes treated with 1,000 μM of metformin (Figure 1J); the addition of 2.5-mM ADP fully restored basal and ATP-linked respiration and augmented maximal respiration capacity and non-mitochondrial respiration (compared Figures 1J–1I). These results suggest that the decreased ADP level is a limiting factor for the reduction of oxygen consumption rate by supra-pharmacological metformin concentrations.

Determination of Metformin Concentration in Mitochondria of Hepatocytes

It has been proposed that supra-pharmacological metformin concentrations can reduce cellular oxygen consumption by inhibiting mitochondrial complex 1 activity (El-Mir et al., 2000; Owen et al., 2000); however, the half inhibitory concentration (IC_{50}) for mitochondrial complex 1 was found to be around 19–66 mM (Bridges et al., 2014; Dykens et al., 2008). Of note, metformin concentrations found in the portal vein following a therapeutic dose are around 40–80 μM (Wilcock and Bailey, 1994), and after the oral administration of ^{14}C-metformin, over 80% of metformin in the liver accumulates in the cytosolic fractions, whereas only small portions of metformin are found in mitochondria (Wilcock et al., 1991). To date, the actual metformin concentrations in mitochondria remain undetermined. We, therefore, developed a method to determine metformin concentrations in intact mitochondria isolated from Hepa1–6 cells treated with ^{14}C-metformin and unlabeled metformin, as we had observed biphasic effects of metformin on mitochondrial respiration not only in primary hepatocytes (Figures 1A and 1B) but also in Hepa1–6 cells (Figures 2A and 2B). As shown in Figure 2C, in Hepa1–6 cells treated with a pharmacological concentration (75 μM) of metformin (Wilcock and Bailey, 1994), metformin concentrations in the large organelles/debris, mitochondria, and cytosolic fractions are around 4.2,4.6, and 38.2 μM, respectively (Figure 2C). About 88% of metformin accumulates in the cytosolic fraction. Unexpectedly, metformin concentrations in the mitochondria of Hepa1–6 cells treated with a supra-pharmacological concentration (1,000 μM) of metformin are around 64.5 μM (Figure 2D), far below the IC_{50} (19–66 mM) for mitochondrial complex 1, whereas metformin concentrations in large organelles/debris and cytosolic fractions are around 37.0 and 996.0 μM, respectively. Additionally, ~90% of metformin accumulates in the cytosolic fractions. To test whether metformin could directly affect mitochondrial complex's activity, we conducted *in vitro* assays and assessed metformin's effect on the complex's activity by using purified mitochondrial complexes. Our results showed that metformin (~1,000 μM) did not directly affect the enzymatic activity of mitochondrial complexes I–V (Figure 2E). The above data suggest that the inhibition of the mitochondrial complexes' activity by supra-pharmacological metformin concentrations is unlikely to be the mechanism responsible for the reduction of oxygen consumption.

Pharmacological Metformin Concentrations Augment Mitochondrial Respiration in Hepatocytes

We found that treatment with pharmacological metformin concentrations (75 μM) (Wilcock and Bailey, 1994) for 22 h significantly suppressed glucose production in primary hepatocytes (Figure 3A) (Cao et al., 2014). This pharmacological metformin concentration (75 μM) significantly increased ATP levels (Figure 3B), mitochondrial membrane potential (Figure 3C), and basal oxygen consumption rate and ATP-linked respiration in primary hepatocytes when pyruvate was used as substrates (Figures 3D and 3E). Treatment with 75 μM of metformin for 3 or 6 h also significantly increased basal oxygen consumption rate and ATP-linked respiration (Figures S1C and S1D) without a reduction in mitochondrial membrane potential (Figure S1E). Furthermore, treatment with 75 μM of metformin significantly increased basal respiration, ATP-linked respiration, maximal respiration capacity, and non-mitochondrial respiration in primary hepatocytes when palmitate and BSA were used as mitochondrial substrates (Figures 3F and 3G). These data indicate that pharmacological metformin concentration increases mitochondrial respiration in hepatocytes.

Metformin Augments Total Mitochondrial Complex 1 Activity in the Liver of HFD-Fed Mice

The maximum approved daily dose of metformin for treatment of patients with T2D is 2.55 g (36 mg/kg body weight), and human studies showed that metformin is able to activate mitochondrial respiratory chain activity (Larsen et al., 2012; Victor et al., 2015). To determine whether metformin at clinically relevant doses can influence blood glucose levels and liver mitochondrial activity in HFD-fed mice, we conducted a series of studies in which different doses of metformin (0, 6.25, 12.5, 25, and 50 mg/kg/day) were given to mice by drinking water after being fed an HFD for 4 weeks. Mice treated with 25 and 50 mg/kg/day of metformin exhibited significantly less gain in body weight and reduced food consumption (Figures 4A and 4B). These data are consistent with the clinical observations of body weight loss and reduction of food intake in metformin-treated patients with T2D (Adeyemo et al., 2015; Knowler et al., 2002).

Treatment with 50 mg/kg/day of metformin significantly decreased glucose production in the liver in a pyruvate challenge experiment (Figure 4C) and improved fasting blood glucose levels (Figure 4D) along with decreased serum levels of insulin and leptin (Figures 4E and 4F). Treatment with 50 mg/kg/day of metformin significantly increased serum gastric inhibitory polypeptide (GIP) levels (Figure 4G). These data support the notion that metformin treatment has an effect on the improvement of insulin sensitivity. Consistent with previous findings in diabetic patients (Doogue et al., 2009), treatment with 50 mg/kg/day of metformin significantly increased serum ghrelin levels (Figure 4H). Because serum ghrelin levels decreased with insulin resistance (Stylianou et al., 2007), the increase in serum ghrelin is another piece of evidence supporting the improvement of insulin sensitivity by metformin.

It has been proposed that inhibition of mitochondrial complex 1 activity is the principal mechanism of metformin’s therapeutic benefits (Foretz et al., 2010). We, therefore, determined total mitochondrial complex 1 activity in the liver in our mice treated with metformin. We found that metformin treatment did not inhibit liver mitochondrial complex 1

activity; rather, treatment with 50 mg/kg/day of metformin significantly increased liver mitochondrial complex 1 activity (Figure 4J). In addition, metformin treatment significantly increased mitochondrial density and mitochondrial DNA levels in the liver of HFD-fed mice (Figures 4K, 4L, and S2D). We found that plasma metformin concentrations are around 18.4 ± 2.6 μM in HFD-fed mice treated with a dose of metformin (50 mg/kg/day).

Metformin Promotes Mitochondrial Fission in Hepatocytes

Because metformin treatment increased mitochondrial number in the liver of HFD-fed mice (Figures 4K and 4L), we determined the mRNA levels of genes related to mitochondrial respiratory chain activity and biogenesis. Metformin treatment (50 mg/kg/day) had a very mild effect on the mRNA levels of genes related to mitochondrial respiratory chain activity (Table S1) and did not significantly affect the mRNA levels of *Pgc-1α, Nrf1/2,* and *mtTfa* (Figure S3A) or the phosphorylation levels of Creb and p38MAPK (Figure 5A), suggesting that metformin augmentation of liver mitochondria is not through the PGC-1α-driven mitochondrial biogenesis pathway.

In order to maintain the mitochondrial population and function, both fusion and fission play critical roles and occur in a repeating and sequential cycle (Liesa and Shirihai, 2013; Youle and van der Bliek, 2012). In agreement with a previous report (Guo et al., 2013), we found that HFD feeding significantly elevated the protein levels of hepatic Opa1 that is important for mitochondrial fusion and decreased Mff phosphorylation (Figure S3B). This would favor mitochondrial fusion. Metformin treatment significantly increased the phosphorylation of AMPKα at T172 (Figures 5A and 5B). Because activated AMPK directly phosphorylates Mff at S155/172, resulting in mitochondrial fission through Drp1 recruitment to mitochondria (Toyama et al., 2016), we found that metformin treatment significantly increased Mff phosphorylation at both S155/172 and the association of Mff with Drp1 (Figures 5A–5C).

In addition, in primary hepatocytes, metformin increased the phosphorylation of AMPKα and Mff (Figures S3C and S3D). Interestingly, metformin treatment led to decreased levels of long-form Opa1 in the liver (Figure 5A). These data suggest that metformin treatment may promote mitochondrial fission to maintain adequate mitochondrial density/numbers. To validate the effects of metformin on mitochondrial fission, we then determined the mitochondrial density in metformin-treated primary hepatocytes by staining with MitoTracker and found that treatment with 75 μM of metformin significantly increased shortened mitochondria and augmented fluorescence intensity by 33% (Figures 5D–5F). Because mitochondrial fission (fragmentation) is associated with increased mitochondrial respiration and nutrient oxidation (Ishihara et al., 2006; Liesa and Shirihai, 2013; Twig et al., 2008), metformin that stimulates mitochondrial fission would increase mitochondrial respiration, as shown in primary hepatocytes treated with pharmacological metformin concentrations (50 and 75 μM) (Figures 1A, 1B, and 3D–3G).

Metformin Augmentation of Mitochondrial Respiratory Activity Is AMPK Dependent

Considering the importance of AMPK in promoting fission (Toyama et al., 2016), we examined mitochondrial density in primary hepatocytes prepared from floxed AMPKα1/2

mice and liver-specific AMPK α1/2 knockout mice (Figure S5A). The loss of AMPK α1/2 subunits led to a reduction of 20% in mitochondrial density (Figures 5G and 5H) and significantly decreased mitochondrial membrane potential (Figures 5I and 5J) and basal respiration, ATP-linked respiration, maximal respiration capacity, and non-mitochondrial respiration (Figures 5K and 5L), indicating compromised mitochondrial respiration. Moreover, the loss of AMPK α1/2 subunits abolished the metformin-stimulated increase in mitochondrial density (Figures 6A and 6B). Because the pharmacological concentration (75 μM) of metformin increased mitochondrial respiration and membrane potential in primary hepatocytes (Figures 3C–3G), we tested further whether AMPK has a role in metformin-mediated activation of mitochondrial respiration in primary hepatocytes prepared from liver-specific AMPKα1/2 knockout mice. We found that treatment with 75 μM of metformin did not increase mitochondrial membrane potential (Figure 6C) and respiration (Figures 6D and 6E) in the absence of AMPKα1/2 subunits. These data suggest that augmentation of mitochondrial density and respiration activity by pharmacological metformin concentration is AMPK dependent.

To substantiate the role of mitochondrial fission in regulating mitochondrial respiration, we determined the effects of blocking mitochondrial fission by the depletion of Drp1, the dynamin-related GTPase for mitochondrial fission on mitochondrial respiration. Primary hepatocytes prepared from liver-specific Drp1 knockout mice (Figure S4A) (Yamada et al., 2018) had significantly decreased mitochondrial respiration (Figures 6F and S4B), along with increased fat accumulation (Figure 6G). Importantly, the pharmacological metformin concentration (75 μM) augmented ATP levels, and mitochondrial membrane potential and fission were lost in the absence of Drp1 (Figures 6H, 6I, and S4C). These data further support that metformin activates mitochondrial respiration through the promotion of mitochondrial fission.

HFD-Fed Mice with Congenital Knockout of Liver AMPKα1/2 Are Resistant to Metformin

To test the importance of liver AMPK in metformin-mediated improvement of hyperglycemia and insulin sensitivity in HFD-fed mice, we generated congenital liver-specific AMPKα1/2 knockout (cL-α1/2 KO) mice by breeding the homozygous floxed AMPKα1/2 mice with Alb-$Cre^{Tg/O}$ mice (Figure S5A). Congenital combined knockout of liver AMPKα1/2 mice produced litters with the expected Mendelian pattern and did not change liver morphology (Figure S5B). We found that cL-α1/2 KO mice exhibited insulin resistance and had increased *Pck1* mRNA levels in the liver (Figures S5E and S5F).

Next, we examined AMPK's role in the improvement of hyperglycemia by metformin. Floxed AMPKα1/2 mice and cL-α1/2 knockout (KO) mice were fed an HFD for 4 weeks to induce insulin resistance (Cao et al., 2017), and then, both groups of mice were given 50 mg/kg/day metformin through drinking water for 12 weeks. Floxed AMPKα1/2 mice and cL-α1/2 KO mice consumed similar amounts of food during 12 weeks of metformin treatment (Figure S5G), but after metformin treatment, male cL-α1/2 KO mice had significantly higher body weight than floxed AMPKα1/2 mice (Figure S5H). Furthermore, both male and female cL-α1/2 KO mice had significantly higher fasting blood glucose levels than floxed AMPKα1/2 mice (Figure 7A), and male cL-α1/2 KO mice had significantly

higher blood glucose levels in a pyruvate challenge experiment (Figure 7B), exhibited insulin resistance (Figure 7C), and had significantly higher mRNA levels of *G6pc* and *Pck1* in the liver (Figure S5K). These results support that liver AMPKα1/2 play a critical role in metformin's control of glucose metabolism.

To further explore the roles of AMPKα1/2 in glucose metabolism in the liver, we used adeno-associated virus (AAV)-thryoxin-binding globulin (TBG)-Cre to specifically KO AMPK α1/2 in the liver of floxed AMPK α1/2 mice after they reached adulthood (Figure 7D) (Cao et al., 2017). After treatment with metformin, HFD-fed adult mice with KO of liver AMPKα1/2 exhibited significantly higher blood glucose levels in a pyruvate challenge experiment (Figure 7E) and had significantly higher liver mRNA levels of *G6pc* and *Pck1* (Figure 7F). Principal-component analysis (PCA) demonstrated that KO of liver AMPKα1/2 markedly changed liver transcriptomic profile (Figures 7G and 7H). KO of liver AMPKα1/2 in adult mice did not significantly affect food intake, body weight, oxygen consumption, CO_2 production, or heat production (Figures S6D–S6K). To ascertain that AMPK α1/2 are critical for metformin suppression of glucose production in hepatocytes, we prepared primary hepatocytes from HFD-fed adult mice with or without KO of liver AMPKα1/2 and treated with metformin (50 mg/kg/day) for 3 weeks. We found that primary hepatocytes isolated from liver-specific AMPKα1/2 KO mice produced significantly more glucose and had significantly higher mRNA levels of *G6pc* and *Pck1* than primary hepatocytes isolated from floxed control mice (Figures 7I–7K and S6L).

AMPKα1 Is the Principal Catalytic Subunit for Metformin Action

To accurately define the role of each AMPKα subunit in metformin action without compensation between AMPKα subunits, we individually re-expressed an exogenous FLAG-tagged AMPKα1 or α2 subunit in the liver of HFD-fed mice with liver-specific KO of AMPKα1/2. However, the loss of AMPKα1/2 also significantly reduced protein levels of AMPKβ1 and γ1 subunits in the liver (Figure 7D). To avoid these confounding decreases in endogenous AMPKβ1 and γ1 protein levels in hepatocytes of liver-specific AMPKα1/2 KO mice, we used AAV expression vectors under a liver-specific TBG promoter to re-express 1.5-fold exogenous FLAG-tagged AMPKβ1, γ1 plus comparable amounts of either FLAG-tagged AMPKα1 or α2 proteins at their corresponding endogenous protein levels in the liver of adult HFD-fed mice with liver-specific AMPKα1/2 KO (Figure 7L). After metformin treatment for 3 weeks, we conducted a pyruvate challenge experiment and found that mice with a loss of either liver AMPKα1 or α2 had higher blood glucose levels than floxed AMPKα1/2 control mice (Figure 7M); however, the loss of liver AMPKα1 had significantly increased liver glucose production, suggesting that AMPKα1 is the principal AMPK catalytic subunit for metformin suppression of liver glucose production.

DISCUSSION

The maximum daily dose of metformin for the treatment of patients with T2D is around 36 mg/kg body weight (He and Wondisford, 2015), and metformin concentrations found in the portal vein following a therapeutic dose are around 40–80 μM (Wilcock and Bailey, 1994). However, high metformin doses (150–500 mg/kg/day) and concentrations (~5 mM) are

widely used in animals or cultured cells, including some of our own studies (Foretz et al., 2010; He et al., 2009). Such high doses (concentrations) of metformin could generate erroneous results for the interrogation of metformin's mechanisms responsible for the improvement of hyperglycemia and insulin sensitivity in patients with T2D and obesity. Human subjects or animal models with insulin resistance have mitochondrial dysfunction (Kelley et al., 2002; Yamada et al., 1975), leading to reductions of nutrients utilization and the intracellular accumulation of lipids and the development of insulin resistance (Samuel and Shulman, 2012). If metformin functions by inhibiting mitochondrial complex 1 activity, this should further aggravate lipid accumulation and insulin resistance, contrary to the widespread clinical observations during metformin therapy in T2D. We found that HFD-fed mice treated with a clinically relevant dose (50 mg/kg/day) of metformin had significantly higher mitochondrial complex 1 activity and mitochondrial density in the liver of HFD-fed mice and pharmacological concentration (75 μM) of metformin significantly increased the activity of the mitochondrial respiratory chain, cellular ATP levels, and mitochondrial membrane potential and density. These results are consistent with clinical observations during metformin therapy that a clinically relevant dose and pharmacological concentrations of metformin augment mitochondrial respiratory chain activity (Larsen et al., 2012; Victor et al., 2015).

Furthermore, we found that there are elevated protein levels of Opa1, impaired AMPK activity, and decreased phosphorylation of Mff in the liver of obese mice. These data suggest that the reduction of mitochondrial density and function in the liver of obese mice may be due to compromised mitochondrial fission that results in an abnormal mitochondrial life cycle. Metformin treatment decreased long-form Opa1 and increased phosphorylation of Mff and recruitment of Drp1 to Mff. Thus, metformin can restore the mitochondrial life cycle by promoting mitochondrial fission, which is significant. Because fission is associated with mitochondrial respiration (Cereghetti et al., 2008; Ishihara et al., 2006; Tanaka et al., 2010) and inhibition of fission by knocking out Drp1 impairs liver function (Yamada et al., 2018), metformin-stimulated fission will increase nutrient oxidation in mitochondria. The continual cycle of fusion and fission is important for mitochondrial quality control, and metformin-stimulated fission will maintain a healthy mitochondrial population by eliminating compromised mitochondria by mitophagy as well (Liesa and Shirihai, 2013).

It has been proposed that liver AMPK is not required for metformin suppression of liver glucose production and improvement of hyperglycemia; however, in that study, control mice and liver-specific AMPKα1/2 KO mice were fed on a regular diet and were administered a single metformin dose (Foretz et al., 2010; Miller et al., 2013). In those mice, blood glucose levels were affected only at an extremely high metformin dose (300 mg/kg) (Foretz et al., 2010). One caveat to metformin administration is that the improvement in glycemic control is observable in diabetic patients after long-term metformin administration rather than after a single metformin administration. We found treatment with 50 mg/kg/day of metformin significantly improved blood glucose levels in HFD-fed mice, and this metformin dose is close to the metformin dose used to treat patients with T2D (He and Wondisford, 2015). We further tested the importance of AMPK in metformin action by knocking out AMPK α1/2 subunits in the liver of mice fed an HFD. We demonstrate that HFD-fed mice with embryonic liver-specific AMPKα1/2 subunit KO had significantly higher fasting blood

glucose levels and produced more glucose than floxed AMPKα1/2 mice after long-term metformin treatment. These data clearly demonstrate that the AMPK is required for metformin's suppression of liver glucose production and improvement of hyperglycemia in HFD-fed mice.

Metformin treatment can improve hepatic metabolism through activation of AMPK (Zang et al., 2004), and mice with mutations of AMPK-targeted phosphorylation sites in acetyl-CoA carboxylase 1 and 2 exhibited insulin resistance (Fullerton et al., 2013). We observed insulin resistance in HFD-fed mice with congenital liver-specific AMPKα1/2 KO, and metformin failed to stimulate mitochondrial fission and respiration in hepatocyte with the loss of AMPK α1/2, suggesting that metformin-augmented mitochondrial respiration and density is AMPK dependent. Collectively, activation of AMPK by metformin will lead to the suppression rate-limiting enzyme gene expression in the gluconeogenic pathway and fatty acid synthesis, along with an increase in fatty acid oxidation through alleviated mitochondrial activity (Fullerton et al., 2013; He et al., 2009; Zang et al., 2004), resulting in an improvement of insulin sensitivity.

In addition to its antidiabetic effects, metformin has received great attention because many studies have shown a reduction in cancer incidence in patients with diabetes mellitus treated with metformin (Evans et al., 2005; Landman et al., 2010; Li et al., 2009). Inhibition of mitochondrial complex 1 activity has been proposed to be the mechanism of metformin's anti-tumor effects (Lee et al., 2019; Saini and Yang, 2018). However, in *in vitro* experiments, metformin's anti-tumor effects are observable only when supra-pharmacological metformin concentrations are used (Lee et al., 2019). The IC_{50} for the purified mitochondrial complex 1 was found to be around 19–66 mM (Bridges et al., 2014; Dykens et al., 2008). It remains unknown how the required high metformin concentrations for inhibition of complex 1 activity can accumulate in mitochondria because there is no metformin transporter in the inner mitochondrial membrane that has been discovered yet. Even if such a high concentration of metformin can be reached in the mitochondria, this would collapse the mitochondrial membrane potential because metformin is positively charged in cells. Because treatment with a supra-pharmacological metformin concentration (1,000 μM) significantly reduced mitochondrial respiration, we determined the mitochondrial metformin concentrations in hepatocytes treated with 1,000 μM of metformin and found that the metformin concentration in mitochondria is around 64.5 μM, two orders of magnitude below the IC_{50} (19–66 μM) for mitochondrial complex 1's activity. Furthermore, we found that supra-pharmacological metformin concentrations (500 and 1,000 μM) suppressed mitochondrial respiration without a reduction in the mitochondrial membrane potential; our results indicate that direct inhibition of mitochondrial complex activity is unlikely to be the mechanism for suppression of mitochondrial respiration by supra-pharmacological metformin concentrations. As the powerhouses of the cell, mitochondria generate ATP from ADP; if ADP is not available, mitochondrial respiration comes to a halt and the mitochondrial membrane potential cannot be utilized to make ATP. This is the case when supra-pharmacological metformin concentrations were used, as cellular ADP was drastically reduced; the addition of exogenous ADP restored mitochondrial respiration suppressed by supra-pharmacological metformin concentrations. Our data suggest that supra-pharmacological metformin concentrations reduce mitochondrial respiration through

decreasing adenine nucleotide levels. Interestingly, supra-pharmacological concentrations of metformin (~200 mM) could not inhibit complex 1's activity in the absence of nucleotides (Bridges et al., 2014), suggesting supra-pharmacological concentrations of metformin may interfere with the binding of nucleotides to the mitochondrial complex. Even though our results showed that treatment with supra-pharmacological metformin concentrations alters the expression of genes related to the metabolism of adenine nucleotides, the detailed mechanism still remains to be elucidated.

STAR★METHODS

LEAD CONTACT AND MATERIALS AVAILIBILITY

Requests for resources and reagents should be directed to and will be fulfilled by the Lead Contact, Ling He (heling@jhmi.edu). This study did not generate new unique reagents.

EXPERIMENTAL MODEL AND SUBJECT DETAILS

All animal protocols were approved by the Institutional Animal Care and Use Committee of the Johns Hopkins University. To test metformin dosage's effects on metabolic parameters, Male C57BL/6J mice at age of 6 weeks were fed an HFD for 4 weeks, then treated with different dose of metformin for 16 weeks through drinking water. Homozygous AMPKα1 mice, homozygous AMPKα2 mice, and albumin promoter-Cre transgenic mice (Alb-$Cre^{Tg/O}$) were purchased from the Jackson Laboratory. We bred homozygous AMPKα1/2 mice with Alb-$Cre^{Tg/O}$, and generated the congenital liver-specific AMPKα1/2 knockout mice. Mice weight gain and water consumption were measured every 7 days, and metformin concentrations in drinking water were adjusted accordingly. AAV8-TBG-Empty vector (E.V.), and AAV8-TBG-Cre (1×10^{11} GC/mouse) were injected into mice through the jugular vein. In an experiment to determine the relative importance of AMPKα1 and α2 in metformin's effect on suppression of liver glucose production, mice were injected with AAV8-TBG-E.V. or AAV8-TBG-Cre (1.5×10^{11} GC/mouse), AAV8-TBG-FLAG-tagged AMPKβ1 (2×10^{12} GC/mouse), AAV8-TBG-FLAG-tagged AMPKγ1 (2×10^{12} GC/mouse), and either AAV8-TBG-FLAG-tagged AMPKα1 (2×10^{12} GC/mouse) or AAV8-TBG-FLAG-tagged AMPKα2 (3×10^{12} GC/mouse) through the jugular vein. The same amounts of AAV (7.15×10^{12} GC/mouse) were employed in each mouse. A pyruvate tolerance test was conducted after 16 h of fast (2 g/kg). An insulin tolerance test was conducted after 6 h of fast (0.5~0.8 unit/kg). A glucose tolerance test was conducted after 6 h of fast (2 g/kg) (He et al., 2016). Floxed DRP1 mice and liver-specific DRP1 knockout mice were generated as reported previously (Yamada et al., 2018).

Cell Culture—Cell culture were conducted using primary hepatocytes or cryopreserved Hepa1–6 cells (ATCC). Please refer to individual sections below and Figure Legends for the specific stimulation condition used for each assay. Cells were incubated in standard conditions: 37° C with 5% CO_2.

METHOD DETAILS

Measurement of Metabolic Hormones, and Mitochondrial Complex 1 Activity—Serum metabolic hormones were determined using a mouse endocrine panel kit (Millipore)

(He et al., 2009). For measurement of mitochondrial complex 1 enzymatic activity, the Mitochondria Isolation Kit for Tissue (with Dounce Homogenizer) (ab110169, abcam) was used to isolate mitochondria from frozen liver tissues following the manufacturer's guidance, and then, mitochondrial complex 1 enzymatic activity was measured by using the Complex I Enzyme Activity Microplate Assay Kit (ab109721, abcam).

Determination of Metformin Concentrations in Cellular Compartments— Hepa1–6 cells were seeded in a 150 cm^2 flask (approximately 1.5×10^7cells/ flask) overnight; medium was changed and supplemented with 2 μM ^{14}C-metformin (Cat#101970, VWR) plus 73 or 998 μM unlabeled metformin for 22 h. Cells were washed with fresh medium, harvested by scraper, and cells were collected by centrifugation (1000 g, 5 min); cell pellets were then washed with PBS twice. A mitochondria isolation kit (ab110171, abcam) was used to prepare the large organelles/debris, intact mitochondria, and cytosolic fractions following the manufacturer's procedures. To measure the volume of the cell pellets, the cell pellets were dissolved into 60 μl of reagent A. The volume was remeasured, and the increase in volume was taken as the volume of cell pellets. After the preparation of large organelles/debris, mitochondria, and cytosolic fractions, the cellular pellets of either large organelles/debris or mitochondria were dissolved into 100 μl of cell lysis buffer. The volumes were remeasured, and the increases in volume were taken as the volumes of large organelles/debris or mitochondria. Then, these lysates were subjected to 3 freeze-thaw cycles (liquid nitrogen), and radioactivity was counted in 5 mL liquid scintillation fluid. The radioactivity of serially diluted ^{14}C-metformin was measured to generate the standard curve. Based on the specific activity of ^{14}C-metformin, metformin concentrations in each cellular compartments were calculated accordingly. Additionally, to validate this method, we treated Hepa1–6 cells with 1 mM of metformin (^{14}C-metformin/unlabeled metformin at 1:250 or 1:500 ratio) for 22 h, and then, cellular fractions were prepared. We found similar concentrations of metformin in each fraction in Hepa1–6 cells treated with these two ^{14}C-metformin/unlabeled metformin ratios.

Glucose Production Assay and Measurement of Mitochondrial Membrane Potential and Cellular Adenine Nucleotide Levels—Mouse primary hepatocytes were cultured in William's medium E supplemented with ITS (BD Biosciences) and dexamethasone. After 16 h of planting, cells were washed with PBS twice, and the medium was changed to FBS-free DMEM. After 3 h of serum starvation, cells were washed twice with PBS, and the 1 mL glucose production medium (20 mM lactate, 2 mM lactate, pH7.4) was supplemented with vehicle or 10 nM glucagon. After 3 h incubation, both the medium and cells were collected. The medium was used to determine glucose concentrations with EnzyChrom Glucose Assay Kit (Cao et al., 2017). For the measurement of mitochondrial membrane potential, primary hepatocytes were stained with TMRE by using Mitochondrial Membrane Potential Assay Kit (ab113852). The intensity of TMRE fluorescence was determined by microplate spectrophotometry and confocal fluorescent microscopy (one z stack was acquired). Cellular ATP, ADP, and AMP levels were determined using methods as we reported previously (Cao et al., 2014)

Determination of Mitochondrial Respiratory Chain Activity in Primary Hepatocytes and *In Vitro* Assays—Primary hepatocytes were seeded in an XF 96 well plate coated with 0.01% collagen type 1.36 h after seeding, cells were washed with PBS twice, and glucose production medium was added with different concentrations of metformin for 6 h. Mitochondrial respiratory chain activity was determined by using Seahorse XF96 Extracellular Flux Analyzers in Seahorse assay medium (0.55 mg/ml pyruvate in base medium, pH7.4). After determination of basal oxygen consumption rates, cells were sequentially treated with oligomycin A (1 μM), FCCP(1 μM), and rotenone (1 μM) along with antimycin A(1 μM). Viable cell numbers were counted and used to normalize the oxygen consumption rate.

Different metformin concentrations were used to determine the effects of metformin on mitochondrial activity of complex I (ab109903, abcam), complex II+III (ab109905, abcam), complex IV (ab109906, abcam), and complex V (ab109907, abcam) in *in vitro* assays following the manufacturer's procedures.

Microarray Analysis—6-week-old male floxed homozygous AMPKα1/2 mice were fed an HFD for 4 weeks. AAV8-TBG-E.V. and AAV8-TBG-Cre were injected via the jugular vein, and mice were treated with metformin (50 mg/kg/day) for 3 weeks. Liver samples were collected after a 16 h fast. Microarray analysis was conducted in the Johns Hopkins Deep Sequencing & Microarray Core Facility.

Oil Red O Staining—Oil Red O (Sigma O0625) was used to stain lipid droplets in primary hepatocytes. Primary hepatocytes were fixed with 4% paraformaldehyde for 30 min, then incubated in 60% isopropanol for 5 min at room temperature, followed by staining with 0.35% Oil red O solution in 60% isopropanol for 15 min and hematoxylin solution (Vector laboratories, H3502) for 1min.

Confocal Microscopy Analysis—Primary hepatocytes were cultured in glucose production medium (20 mM lactate and 2 mM pyruvate) with or without 75 uM metformin for 6 h, and then, 50 nM MitoTracker™ Red FM (M22425, Thermo Fisher Scientific) was added for 30 min, followed by addition of Hoechst33342 (2 ug/ml, 10 min) (H3570, Thermo Fisher Scientific). Fluorescent images were acquired via a Zeiss confocal microscope (Zeiss Confocal LSM 880). The excitation wavelengths of MitoTracker™ Red CMR and Hoechst33342 are at 561 nm and 405 nm, respectively. 12 z stacks were acquired, and then merged by Zeiss Zen software.

Quantification of Mitochondrial DNA Copy Number—DNeasy Blood & Tissue Kit (69504, QIAGEN) was used to extract genomic DNA from liver tissues. A mitochondrial DNA isolation kit (ab65321, abcam) was employed to prepare the mitochondrial DNA from liver tissues. The following primer sequences were used to amplify nuclear and mitochondrial DNA sequences: PKLR 5′-CCAGCAGCATCAGTCGTATATC, PKLR 3′-ACCCAGGAGGAATC GAATTAAC; ND6 5′-GTTTGGGAGATTGGTTGATGTATG, ND6 3′-CACCCAGCTACTACCATCATTC.

Indirect Calorimetry—Mice were allowed to acclimate to respiratory chambers for 24 h. Oxygen consumption, carbon dioxide production, heat production, and food consumption were measured for 48 h during 12-h light/12-dark cycles using the Comprehensive Lab Animal Monitoring System (CLAMS) (Columbus Instruments, Columbus, OH).

Transmission Electron Microscopy (TEM)—Liver tissue was cut at 10 μm and sections were fixed in ice cold 0.1 M Sorenson's phosphate buffer (pH 7.2) (2.5% glutaraldehyde, 3mM $MgCl_2$) for 15 minutes. After rinse with buffer, tissue sections were post-fixed in 0.8% potassium ferrocyanide for 30 minutes on ice in the dark, followed by 0.1 M maleate buffer rinse. Then, tissue sections were stained with 2% uranyl acetate (0.22 μm filtered, 15 minutes, dark) in 0.1 M maleate, dehydrated in a graded series of ethanol, and embedded in Eponate 12 (Ted Pella). Tissue sections were polymerized overnight in inverted BEEM capsules and immersed in liquid nitrogen. Thin sections, 60 to 90 nm, were cut with a diamond knife on a Leica UCT7 ultramicrotome and picked up with Formvar coated copper slot grids. Grids were stained with 2% uranyl acetate in 50% methanol and observed with a Philips CM120 at 80 kV. Images were captured with an AMT XR80 high-resolution (16-bit) 8 M pixel camera. 13–18 fields were randomly chosen from each liver section and were used to count mitochondria number.

QUANTIFICATION AND STATISTICAL ANALYSIS

Statistical significance was calculated with a Student's t test. Significance was accepted at the level of $p < 0.05$. At least 3 samples per group were chosen for statistically meaningful interpretation of results and differences in the studies using the two-tailored Student's t test and analysis of variation. Multiple-way comparisons were performed using ANOVA. Statistical analyses were performed using GraphPad Prism.

DATA AND CODE AVAILABILITY

The Data for this study have been deposited in GEO with accession codee: GSE 114234

Supplementary Material

Refer to Web version on PubMed Central for supplementary material.

ACKNOWLEDGMENTS

This work was supported in part by grants from the NIH: R01DK107641 (L.H.), R01DK120309 (L.H.), and GM123266 (H.S.). We thank Barbara Smith in the Cell Biology Facility at Johns Hopkins School of Medicine for helping with the confocal microscope and transmission electron microscopy.

REFERENCES

Adeyemo MA, McDuffie JR, Kozlosky M, Krakoff J, Calis KA, Brady SM, and Yanovski JA (2015). Effects of metformin on energy intake and satiety in obese children. Diabetes Obes. Metab 17, 363–370. [PubMed: 25483291]

Bridges HR, Jones AJ, Pollak MN, and Hirst J (2014). Effects of metformin and other biguanides on oxidative phosphorylation in mitochondria. Biochem. J 462, 475–487. [PubMed: 25017630]

Cao J, Meng S, Chang E, Beckwith-Fickas K, Xiong L, Cole RN, Radovick S, Wondisford FE, and He L (2014). Low concentrations of metformin suppress glucose production in hepatocytes through AMP-activated protein kinase (AMPK). J. Biol. Chem 289, 20435–20446. [PubMed: 24928508]

Cao J, Peng J, An H, He Q, Boronina T, Guo S, White MF, Cole PA, and He L (2017). Endotoxemia-mediated activation of acetyltransferase P300 impairs insulin signaling in obesity. Nat. Commun 8, 131. [PubMed: 28743992]

Cereghetti GM, Stangherlin A, Martins de Brito O, Chang CR, Blackstone C, Bernardi P, and Scorrano L (2008). Dephosphorylation by calcineurin regulates translocation of Drp1 to mitochondria. Proc. Natl. Acad. Sci. USA 705, 15803–15808.

Cheng Z, Guo S, Copps K, Dong X, Kollipara R, Rodgers JT, Depinho RA, Puigserver P, and White MF (2009). Foxo1 integrates insulin signaling with mitochondrial function in the liver. Nat. Med 75, 1307–1311.

Cheng Z, Tseng Y, and White MF (2010). Insulin signaling meets mitochondria in metabolism. Trends Endocrinol. Metab 27, 589–598.

Doogue MP, Begg EJ, Moore MP, Lunt H, Pemberton CJ, and Zhang M (2009). Metformin increases plasma ghrelin in Type 2 diabetes. Br. J. Clin. Pharmacol 88, 875–882.

Dykens JA, Jamieson J, Marroquin L, Nadanaciva S, Billis PA, and Will Y (2008). Biguanide-induced mitochondrial dysfunction yields increased lactate production and cytotoxicity of aerobically-poised HepG2 cells and human hepatocytes in vitro. Toxicol. Appl. Pharmacol 288, 203–210.

El-Mir MY, Nogueira V, Fontaine E, Avéret N, Rigoulet M, and Leverve X (2000). Dimethylbiguanide inhibits cell respiration via an indirect effect targeted on the respiratory chain complex I. J. Biol. Chem 275, 223–228. [PubMed: 10617608]

Evans JM, Donnelly LA, Emslie-Smith AM, Alessi DR, and Morris AD (2005). Metformin and reduced risk of cancer in diabetic patients. BMJ 880, 1304–1305.

Foretz M, Hébrard S, Leclerc J, Zarrinpashneh E, Soty M, Mithieux G, Sakamoto K, Andreelli F, and Viollet B (2010). Metformin inhibits hepatic gluconeogenesis in mice independently of the LKB1/AMPK pathway via a decrease in hepatic energy state. J. Clin. Invest 720, 2355–2369.

Fullerton MD, Galic S, Marcinko K, Sikkema S, Pulinilkunnil T, Chen ZP, O'Neill HM, Ford RJ, Palanivel R, O'Brien M, et al. (2013). Single phosphorylation sites in Acc1 and Acc2 regulate lipid homeostasis and the insulin-sensitizing effects of metformin. Nat. Med 79, 1649–1654.

Guo Y, Darshi M, Ma Y, Perkins GA, Shen Z, Haushalter KJ, Saito R, Chen A, Lee YS, Patel HH, et al. (2013). Quantitative proteomic and functional analysis of liver mitochondria from high fat diet (HFD) diabetic mice. Mol. Cell. Proteomics 72, 3744–3758.

Hardie DG, Ross FA, and Hawley SA (2012). AMPK: a nutrientand energy sensor that maintains energy homeostasis. Nat. Rev. Mol. Cell Biol 78, 251–262.

Hawley SA, Gadalla AE, Olsen GS, and Hardie DG (2002). The antidiabetic drug metformin activates the AMP-activated protein kinase cascade via an adenine nucleotide-independent mechanism. Diabetes 57, 2420–2425.

He L, and Wondisford FE (2015). Metformin action: concentrations matter Cell Metab. 27, 159–162.

He L, Chang E, Peng J, An H, McMilin SM, Radovick S, Stratakis CA, and Wondisford FE (2016). Activation of the cAMP-PKA pathway antagonizes metformin suppression of hepatic glucose production. J. Biol. Chem 297, 10562–10570.

He L, Sabet A, Djedjos S, Miller R, Sun X, Hussain MA, Radovick S, and Wondisford FE (2009). Metformin and insulin suppress hepatic gluconeogenesis through phosphorylation of CREB binding protein. Cell 787, 635–646.

He L, Meng S, Germain-Lee EL, Radovick S, and Wondisford FE (2014). Potential biomarker of metformin action. J. Endocrinol 227, 363–369.

Hundal RS, Krssak M, Dufour S, Laurent D, Lebon V, Chandramouli V, Inzucchi SE, Schumann WC, Petersen KF, Landau BR, and Shulman GI (2000). Mechanism by which metformin reduces glucose production in type 2 diabetes. Diabetes 49, 2063–2069. [PubMed: 11118008]

Ishihara N, Fujita Y, Oka T, and Mihara K (2006). Regulation of mitochondrial morphology through proteolytic cleavage of OPA1. EMBO J. 25, 2966–2977. [PubMed: 16778770]

Kelley DE, He J, Menshikova EV, and Ritov VB (2002). Dysfunction of mitochondria in human skeletal muscle in type 2 diabetes. Diabetes 51, 2944–2950. [PubMed: 12351431]

Knowler WC, Barrett-Connor E, Fowler SE, Hamman RF, Lachin JM, Walker EA, and Nathan DM; Diabetes Prevention Program Research Group (2002). Reduction in the incidence oftype 2 diabetes with lifestyle intervention or metformin. N. Engl. J. Med 346, 393–403. [PubMed: 11832527]

Landman GW, Kleefstra N, van Hateren KJ, Groenier KH, Gans RO, and Bilo HJ (2010). Metformin associated with lower cancer mortality in type 2 diabetes: ZODIAC-16. Diabetes Care 33, 322–326. [PubMed: 19918015]

Larsen S, Rabøl R, Hansen CN, Madsbad S, Helge JW, and Dela F (2012). Metformin-treated patients with type 2 diabetes have normal mitochondrial complex I respiration. Diabetologia 55, 443–449. [PubMed: 22009334]

Lee H, and Yoon Y (2014). Transient contraction of mitochondria induces depolarization through the inner membrane dynamin OPA1 protein. J. Biol. Chem 289, 11862–11872. [PubMed: 24627489]

Lee YJ, Jeschke GR, Roelants FM, Thorner J, and Turk BE (2012). Reciprocal phosphorylation of yeast glycerol-3-phosphate dehydrogenases in adaptation to distinct types of stress. Mol. Cell. Biol 32, 4705–4717. [PubMed: 22988299]

Lee J, Yesilkanal AE, Wynne JP, Frankenberger C, Liu J, Yan J, Elbaz M, Rabe DC, Rustandy FD, Tiwari P, et al. (2019). Effective breast cancer combination therapy targeting BACH1 and mitochondrial metabolism. Nature 568, 254–258. [PubMed: 30842661]

Li D, Yeung SC, Hassan MM, Konopleva M, and Abbruzzese JL (2009). Antidiabetic therapies affect risk of pancreatic cancer. Gastroenterology 137, 482–488. [PubMed: 19375425]

Liesa M, and Shirihai OS (2013). Mitochondrial dynamics in the regulation of nutrient utilization and energy expenditure. Cell Metab. 17, 491–506. [PubMed: 23562075]

Madiraju AK, Erion DM, Rahimi Y, Zhang XM, Braddock DT, Albright RA, Prigaro BJ, Wood JL, Bhanot S, MacDonald MJ, et al. (2014). Metformin suppresses gluconeogenesis by inhibiting mitochondrial glycerophosphate dehydrogenase. Nature 510, 542–546. [PubMed: 24847880]

Meng S, Cao J, He Q, Xiong L, Chang E, Radovick S, Wondisford FE, and He L (2015). Metformin activates AMP-activated protein kinase by promoting formation of the αβγ heterotrimeric complex. J. Biol. Chem 290, 3793–3802. [PubMed: 25538235]

Miller RA, Chu Q, Xie J, Foretz M, Viollet B, and Birnbaum MJ (2013). Biguanides suppress hepatic glucagon signalling by decreasing production of cyclic AMP. Nature 494, 256–260. [PubMed: 23292513]

Morino K, Petersen KF, Dufour S, Befroy D, Frattini J, Shatzkes N, Neschen S, White MF, Bilz S, Sono S, et al. (2005). Reduced mitochondrial density and increased IRS-1 serine phosphorylation in muscle of insulin-resistant offspring oftype 2 diabetic parents. J. Clin. Invest 115, 3587–3593. [PubMed: 16284649]

Owen MR, Doran E, and Halestrap AP (2000). Evidence that metformin exerts itsanti-diabetic effectsthrough inhibition ofcomplex 1 ofthe mitochondrial respiratory chain. Biochem. J 348, 607–614. [PubMed: 10839993]

Petersen KF, Dufour S, Befroy D, Garcia R, and Shulman GI (2004). Impaired mitochondrial activity in the insulin-resistant offspring of patients with type 2 diabetes. N. Engl. J. Med 350, 664–671. [PubMed: 14960743]

Ritov VB, Menshikova EV, He J, Ferrell RE, Goodpaster BH, and Kelley DE (2005). Deficiency of subsarcolemmal mitochondria in obesity and type 2 diabetes. Diabetes 54, 8–14. [PubMed: 15616005]

Saini N, and Yang X (2018). Metformin as an anti-cancer agent: actions and mechanisms targeting cancer stem cells. Acta Biochim. Biophys. Sin. (Shanghai) 50, 133–143. [PubMed: 29342230]

Samuel VT, and Shulman GI (2012). Mechanisms for insulin resistance: common threads and missing links. Cell 148, 852–871. [PubMed: 22385956]

Shaw RJ, Lamia KA, Vasquez D, Koo SH, Bardeesy N, Depinho RA, Montminy M, and Cantley LC (2005). The kinase LKB1 mediates glucose homeostasis in liver and therapeutic effects of metformin. Science 310, 1642–1646. [PubMed: 16308421]

Stylianou C, Galli-Tsinopoulou A, Farmakiotis D, Rousso I, Karamouzis M, Koliakos G, and Nousia-Arvanitakis S (2007). Ghrelin and leptin levels in obese adolescents. Relationship with body fat and insulin resistance. Hormones (Athens) 6, 295–303. [PubMed: 18055420]

Takashima M, Ogawa W, Hayashi K, Inoue H, Kinoshita S, Okamoto Y, Sakaue H, Wataoka Y, Emi A, Senga Y, et al. (2010). Role of KLF15 in regulation of hepatic gluconeogenesis and metformin action. Diabetes 59, 1608–1615. [PubMed: 20393151]

Tanaka A, Cleland MM, Xu S, Narendra DP, Suen DF, Karbowski M, and Youle RJ (2010). Proteasome and p97 mediate mitophagy and degradation of mitofusins induced by Parkin. J. Cell Biol 191, 1367–1380. [PubMed: 21173115]

Toyama EQ, Herzig S, Courchet J, Lewis TL Jr., Loson OC, Hellberg K, Young NP, Chen H, Polleux F, Chan DC, and Shaw RJ (2016). Metabolism. AMP-activated protein kinase mediates mitochondrial fission in response to energy stress. Science 351, 275–281. [PubMed: 26816379]

Twig G, Elorza A, Molina AJ, Mohamed H, Wikstrom JD, Walzer G, Stiles L, Haigh SE, Katz S, Las G, et al. (2008). Fission and selective fusion govern mitochondrial segregation and elimination by autophagy. EMBOJ. 27, 433–446.

Victor VM, Rovira-Llopis S, Barñuls C, Diaz-Morales N, Castelló R, Falcón R, Gómez M, Rocha M, and Hernández-Mijares A (2015). Effects of metformin on mitochondrial function of leukocytes from polycystic ovary syndrome patients with insulin resistance. Eur. J. Endocrinol 173, 683–691. [PubMed: 26320144]

Wheaton WW, Weinberg SE, Hamanaka RB, Soberanes S, Sullivan LB,Anso E, Glasauer A, Dufour E, Mutlu GM, Budigner GS, and Chandel NS (2014). Metformin inhibits mitochondrial complex I of cancer cells to reduce tumorigenesis. eLife 3, e02242. [PubMed: 24843020]

Wilcock C, and Bailey CJ (1994). Accumulation of metformin by tissues of the normal and diabetic mouse. Xenobiotica 24, 49–57. [PubMed: 8165821]

Wilcock C, Wyre ND, and Bailey CJ (1991). Subcellular distribution of metformin in rat liver. J. Pharm. Pharmacol 43, 442–444. [PubMed: 1681061]

Yamada T, Ida T, Yamaoka Y, Ozawa K, Takasan H, and Honjo I (1975). Two distinct patterns of glucose intolerance in icteric rats and rabbits. Relationship to impaired liver mitochondria function. J. Lab. Clin. Med 86, 38–45. [PubMed: 1151141]

Yamada T, Murata D, Adachi Y, Itoh K, Kameoka S, Igarashi A, Kato T, Araki Y, Huganir RL, Dawson TM, et al. (2018). Mitochondrial Stasis Reveals p62-Mediated Ubiquitination in Parkin-Independent Mitophagy and Mitigates Nonalcoholic Fatty Liver Disease. Cell Metab 28, 588–604.e585. [PubMed: 30017357]

Youle RJ, and van der Bliek AM (2012). Mitochondrial fission, fusion, and stress. Science 337, 1062–1065. [PubMed: 22936770]

Zang M, Zuccollo A, Hou X, Nagata D, Walsh K, Herscovitz H, Brecher P, Ruderman NB, and Cohen RA (2004). AMP-activated protein kinase is required for the lipid-lowering effect of metformin in insulin-resistant human HepG2 cells. J. Biol. Chem 279, 47898–7905. [PubMed: 15371448]

Zhou G, Myers R, Li Y, Chen Y, Shen X, Fenyk-Melody J, Wu M, Ventre J, Doebber T, Fujii N, et al. (2001). Role of AMP-activated protein kinase in mechanism of metformin action. J. Clin. Invest 108, 1167–1174. [PubMed: 11602624]

Highlights

- Clinically relevant metformin dose improves liver mitochondrial respiration in obesity
- Pharmacological metformin increases mitochondrial respiration and fission
- Supra-pharmacological metformin inhibits mitochondrial activity by ADP reduction
- AMPK is required for metformin suppression of liver glucose production

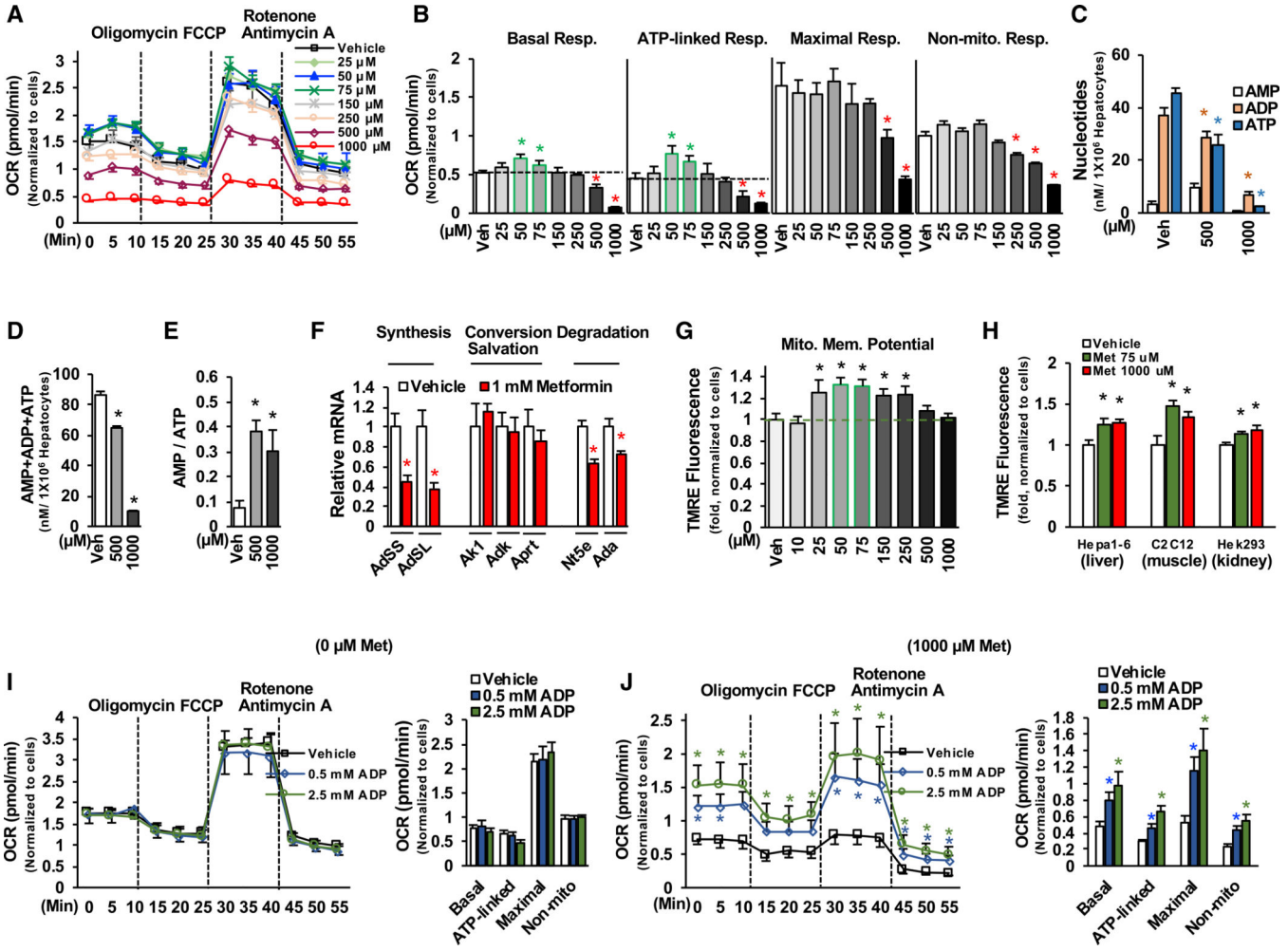

Figure 1. Supra-pharmacological Metformin Concentrations Reduce Adenine Nucleotides and Mitochondrial Respiration

(A and B) After24 h of planting, primary hepatocytes were treated with different concentrations of metformin for16h in DMEM, and then medium was changed to glucose production medium supplemented with metformin for 6 h (A). After determination of basal oxygen consumption rate (OCR), cells were sequentially treated with oligomycin A (1 μM), carbonyl cyanide 4-(trifluoromethoxy)phenylhydrazone (FCCP; 1 μM), and rotenone (1 μM) plus antimycin A(1 μM) (B) (n = 8–10).

(C–E) Primary hepatocytes were treated with 500 and 1,000 μM of metformin as in (A), adenine nucleotides were measured (C), total adenine nucleotides (D), and AMP/ATP ratio (E) (n = 4).

(F) The mRNA levels of genes related to the metabolism of adenine nucleotides in primary hepatocytes treated with 1,000 μM metformin for 22 h (n = 5–6).

(G) Primary hepatocytes were treated with different concentrations of metformin for 22 h (n = 8).

(H) Hepa1–6 cells, C2C12 cells, and Hek293 cells were treated with 75 and 1,000 μM of metformin for 22 h and then stained with tetramethylrhodamine, ethyl ester (TMRE) (n = 6–8).

(I and J) Primary hepatocytes were treated with vehicle (I) or 1,000 μM of metformin (J) as in (A); 0.5 and 2.5 mM of ADP were added in the assay buffer during the measurement of OCR (n = 6–8).

Each bar represents the mean ± SEM. *p < 0.05.

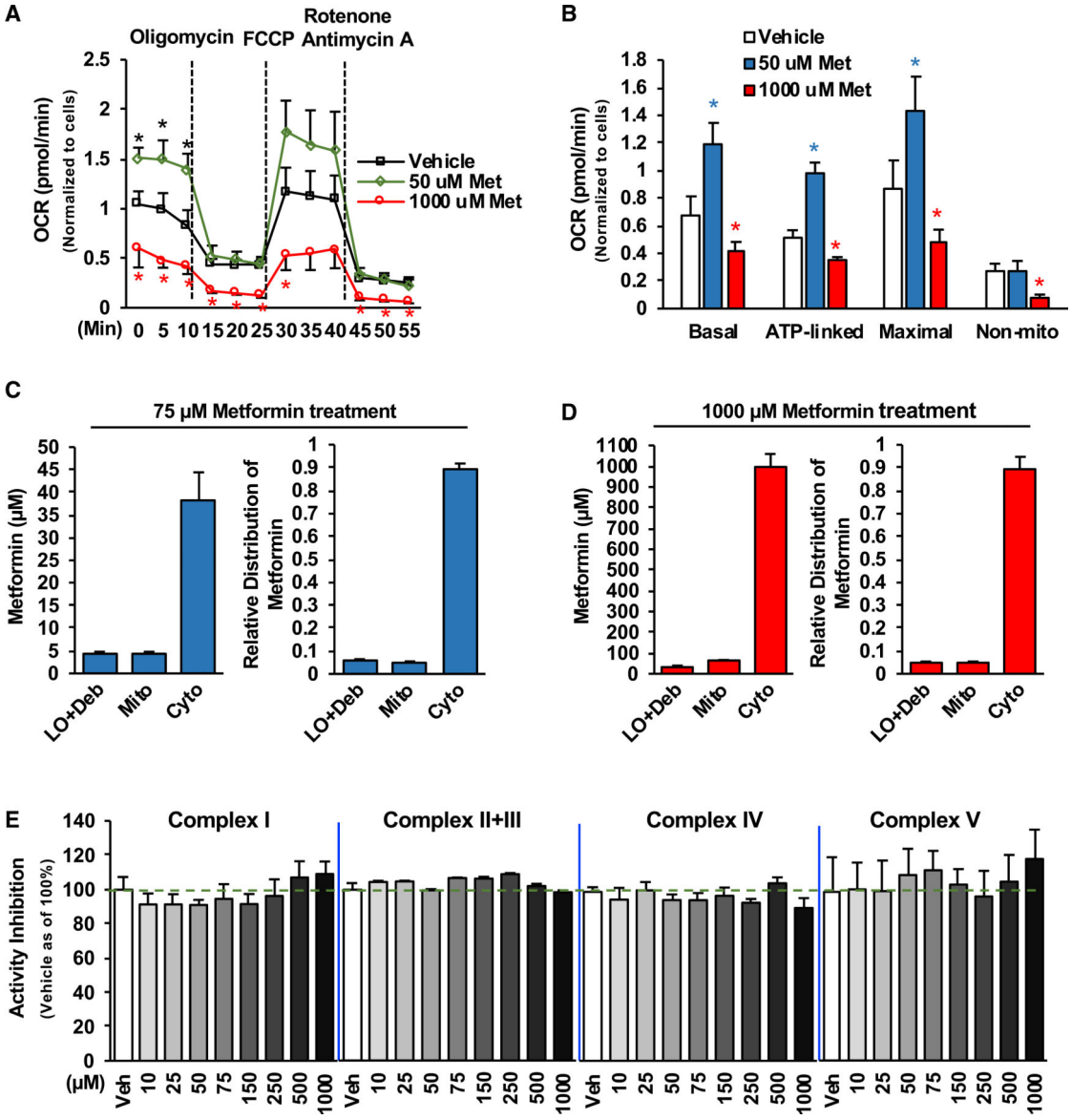

Figure 2. Determination of Metformin Concentrations in Cellular Compartments of Hepatocytes

(A and B) Hepa1–6 cells were treated with different concentrations of metformin as In Figure 1A, and OCR was determined (n = 6–8).

(C and D) Metformin concentrations in the large organelles/debris (LO/Deb), mitochondria (Mito), and cytosolic (Cyto) fractions prepared from Hepa1–6 cells treated with 75 μM (C) (n = 4) or 1,000 μM (D) (n = 5) of metformin for 22 h.

(E) Indicated concentrations of metformin were used to test metformin's effect on mitochondrial activity of complex I, complex II+III, complex IV, and complex V (purchased from the *abcam)* in *in vitro* assays (n = 6–8).

Each bar represents the mean ± SEM. *p < 0.05.

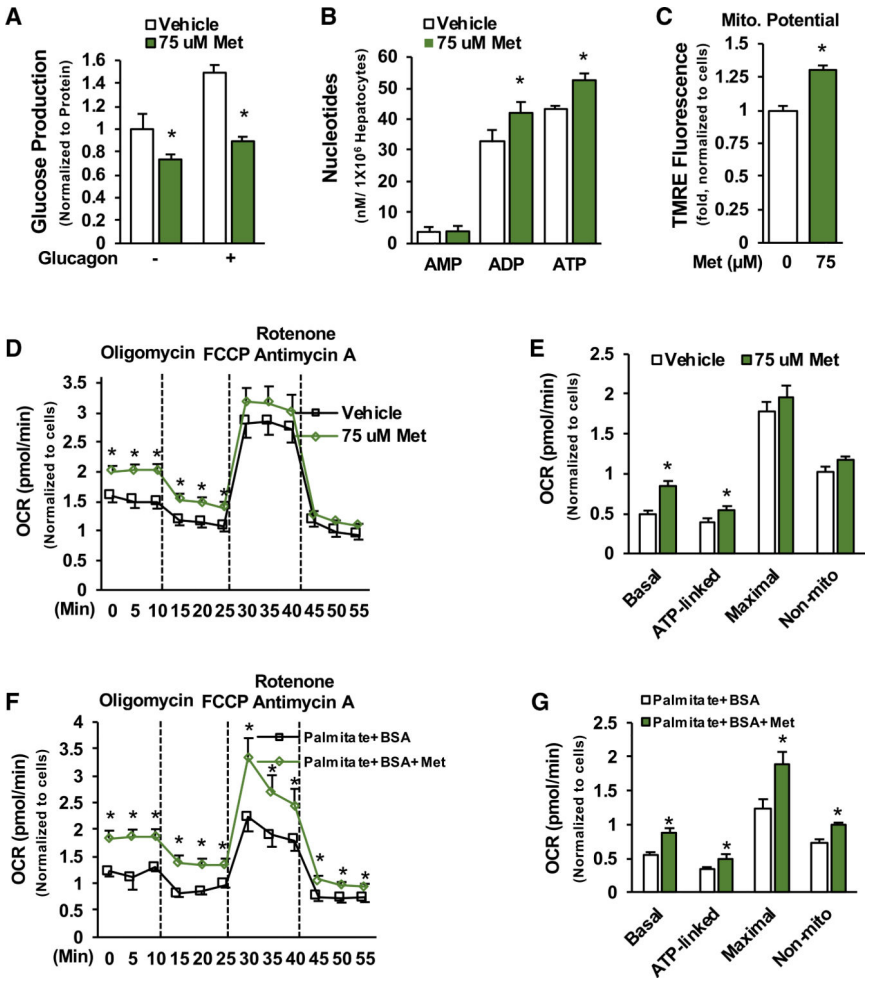

Figure 3. Pharmacological Metformin Concentration Augments Mitochondrial Respiration

(A–C) Primary hepatocytes were treated with 75 μM metformin for 16 h and then treated with metformin for 3 h during serum starvation, followed by incubation in glucose production medium supplemented with metformin and/or 10 nM glucagon for another 3 h. Glucose concentrations were measured in the medium (A) (n = 3), cellular ATP levels (B) (n = 4), and mitochondrial membrane potential (C) (n = 8).

(D and E) Primary hepatocytes were treated with metformin as in Figure 1A (D), and OCR was determined (E) (n = 10).

(F and G) After 24 h of plating, primary hepatocytes were treated with 75 μM metformin for 16 h in substrate-limited medium, and then medium was replaced by fatty acid oxidation assay buffer (palmitate plus BSA) (F), and OCR was determined as above (G) (n = 6–7). Each bar represents the mean ± SEM. *$p < 0.05$.

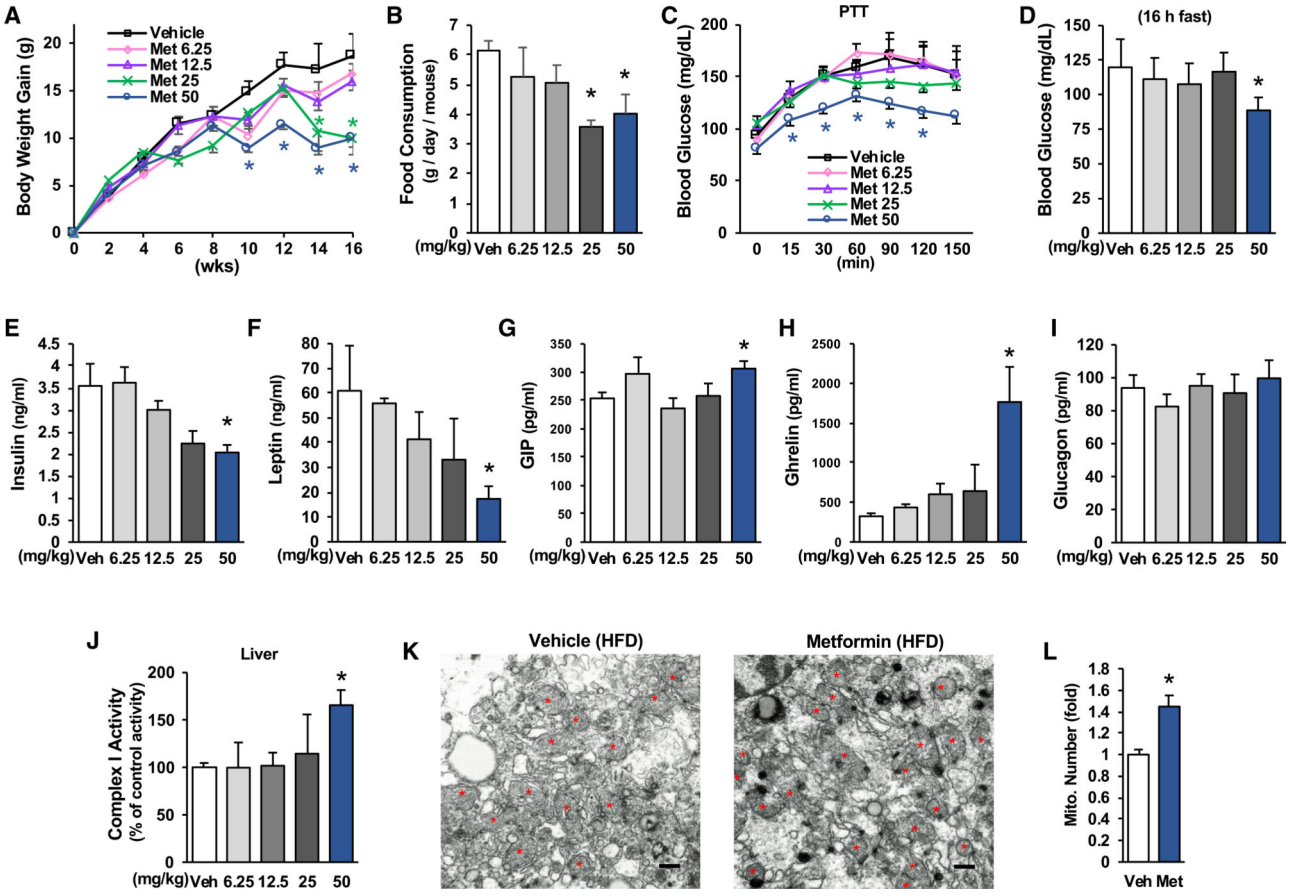

Figure 4. Metformin Improves Metabolic Parameters in HFD-Fed Mice

HFD-fed C57BL/6 mice were divided into 5 groups and treated with indicated amounts of metformin by drinking water for 16 weeks (n = 5–8).

(A) Body weight gain of mice during 16 weeks of metformin treatment.

(B) Food consumption was measured during Comprehensive Lab Animal Monitoring System (CLAMS) (n = 4).

(C) After 9 weeks of metformin treatment, a pyruvate tolerance test was conducted (16 h fast) (n = 5–8).

(D) Fasting blood glucose (16 h fast) in mice after 12 weeks of metformin treatment.

(E–I) Serum levels of insulin (E), leptin (F), GIP (G), ghrelin (H), and glucagon (I) in mice treated with metformin for 16 weeks (n = 5–8).

(J–L) Mitochondrial complex 1 activity (J) (n = 5–8), mitochondrial numbers in the liver (K) (Scale bar, 500 nm), and relative mitochondrial density (L) in HFD-fed mice treated with metformin (50 mg/kg/day) for 16 weeks (n = 4).

Each bar represents the mean ± SEM. *p < 0.05.

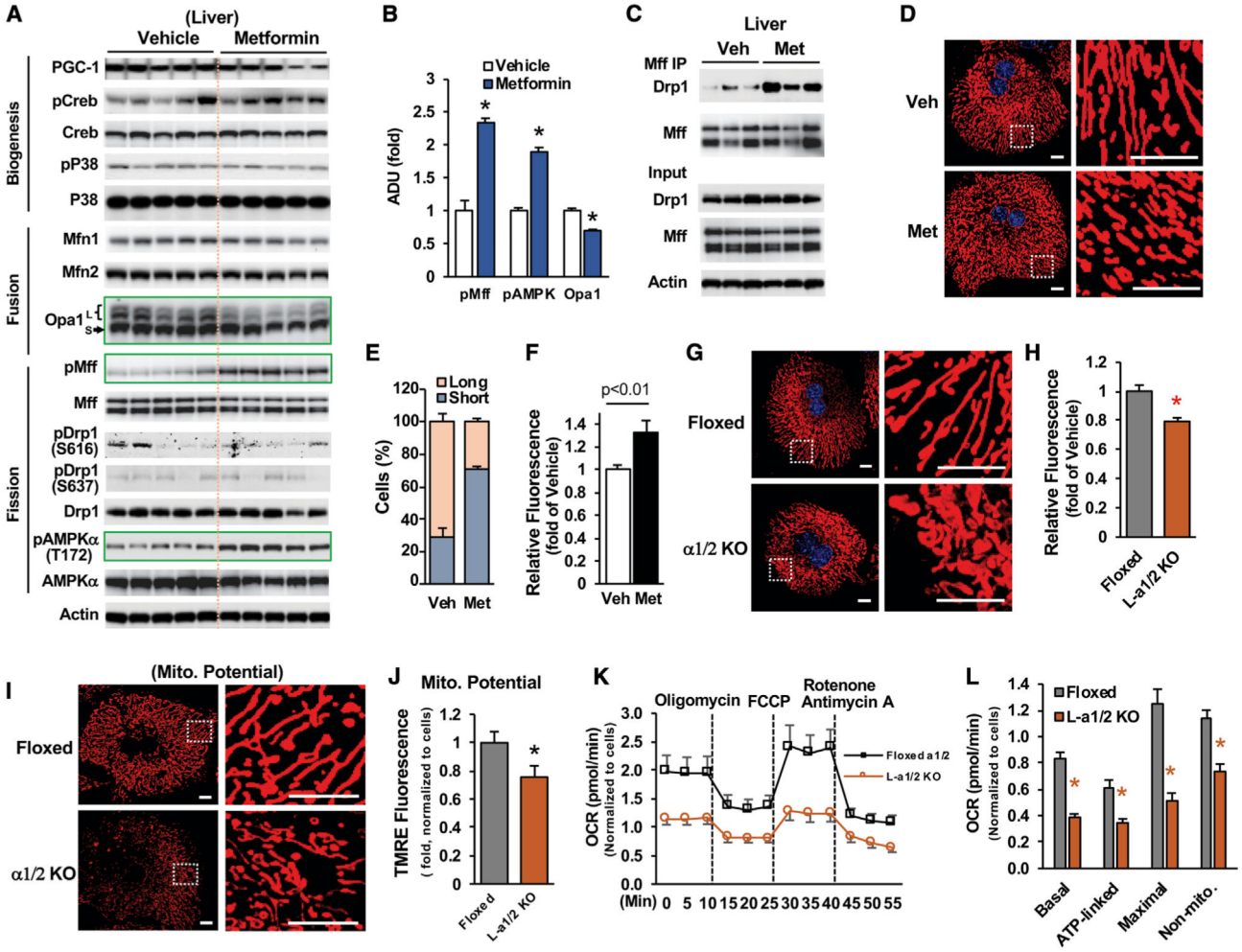

Figure 5. Metformin Promotes Mitochondrial Fission

(A and B)The protein and phosphorylation levels of genes related to mitochondrial biogenesis, fusion, and fission (A) (n = 5), and densitometric analysis of pAMPK (T172), pMff (S155/172), and Opa1 (B).

(C) Liver lysates from HFD-fed mice treated with vehicle and 50 mg/kg/day of metformin were incubated with antibody against Mff (16 h, 4°C) (n = 3).

(A and C) Each lane represents an individual mouse sample.

(D–F) After 24 h of plating, primary hepatocytes prepared from floxed AMPK α1/2 mice were treated with or without 75 uM of metformin for 16 h, medium was changed to glucose production medium supplemented with metformin for 6 h, and then mitochondria were stained with MitoTracker Red (D); relative numbers of cells with indicated mitochondrial morphology (long or short) (E) (n = 119–127); and fluorescence intensity (mitochondrial mass) from 35 cells were measured from each group (F).

(G and H) After 24 h of plating, primary hepatocytes prepared from floxed and liver-specific AMPK α1/2 knockout (L- α1/2 KO) mice were incubated with DMEM for 16 h, medium was changed to glucose production medium for 6 h, and then cells were stained with MitoTracker Red (G); fluorescence intensity (mitochondrial mass) was determined (H) (n = 37).

(I and J) Primary hepatocytes prepared from floxed and L-α1/2 KO mice were stained with TMRE (I) to determine mitochondrial membrane potential (J) (n = 20~26).
(K and L) After 36 h of plating, cellular respiration (K), basal OCR, ATP-linked respiration, maximal respiration, and non-mitochondrial respiration (L) were determined in primary hepatocytes prepared from floxed and L- α1/2 KO mice (n = 5–6).
Scale bar, 10 μm. Each bar represents the mean ± SEM. *$p < 0.05$.

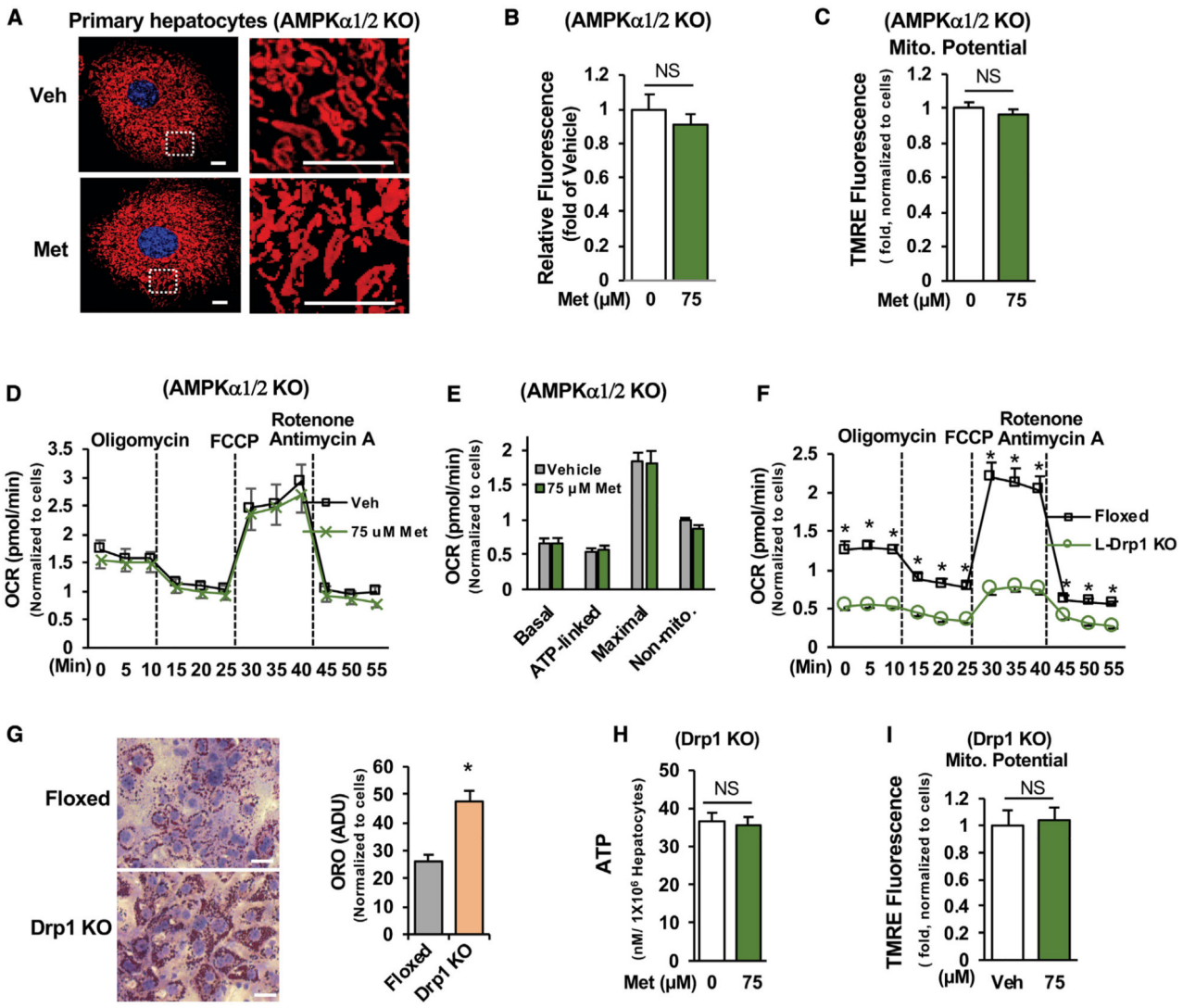

Figure 6. Metformin Stimulation of Mitochondrial Respiration Is AMPK Dependent

(A–C) Primary hepatocytes prepared from L- α1/2 KO mice were treated with metformin as in Figure 5D (A), fluorescence intensity of 40 cells were measured (B), and mitochondrial membrane potential was determined (C) (n = 6). Scale bar, 10 μm.

(D and E) Primary hepatocytes prepared from liver-specific AMPK α1/2 KO mice were treated with vehicle and 75 μM metformin as in Figure 3D (D); OCR was determined (E) (n = 8–10).

(F) OCRs were determined in primary hepatocytes prepared from floxed or liver-specific Drp1 KO mice as above (n = 6).

(G) After 48 h of the planting, primary hepatocytes were stained with Oil Red O, and lipid droplets were measured (n = 91). Scale bar, 50 μM.

(H and I) For measurement of ATP (H) (n = 4) and membrane potential (I) (n = 8), primary hepatocytes were treated as in Figures 3B and 3C.

NS, not significant. Each bar represents the mean ± SEM. *p < 0.05.

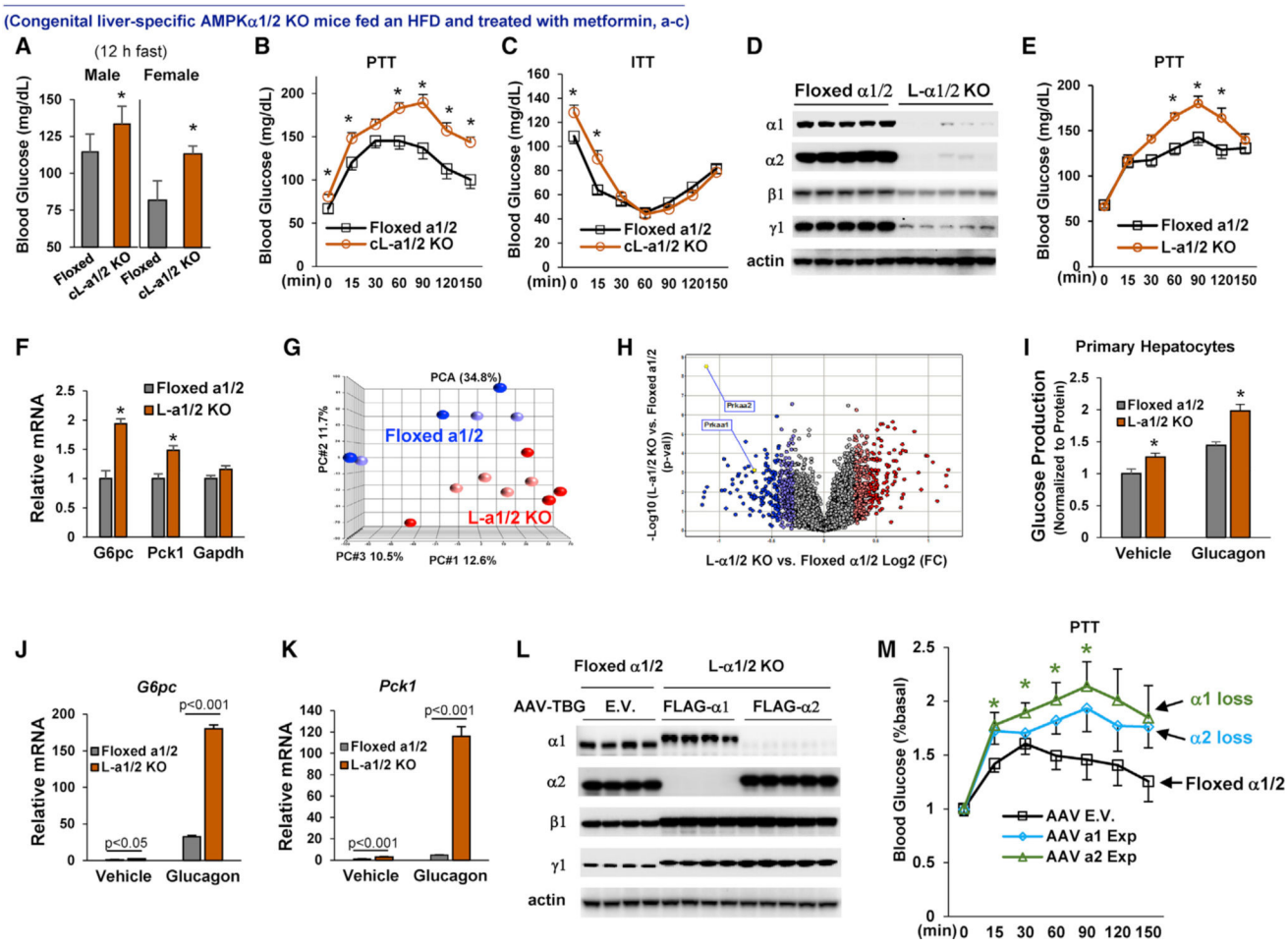

Figure 7. The Critical Role of AMPKα1/2 in Metformin's Control of Liver Glucose Metabolism

(A) Male (n = 9–10) and female (n = 5) mice were fed an HFD for 4 weeks and then treated with metformin (50 mg/kg/day) for12 weeks; 12-h fasting blood glucose levels. The y axis has been broken and begins at 50 mg/dL.

(B and C) HFD-fed male mice were treated with metformin (50 mg/kg/day) for7–9 weeks; pyruvate tolerance test (B) and insulin tolerance test (C) were conducted (n = 6–9).

(D–H) Male floxed AMPKα1/2 mice were fed an HFD for4weeks, AAV-TBG vectors were injected, and then mice were treated with metformin (50 mg/kg/day) for 3 weeks (D).

(E and F) Pyruvate tolerance test (E) and hepatic mRNA levels of *G6pc and Pck1* (F) (n = 5–6).

(G and H) PCA (G) and Volcano plots (H) were used to depict differential expression of liver genes. Data shown are replicated from 2 independent experiments.

(I–K) Primary hepatocytes were isolated from the liver of mice as in (D) and were treated with 10 nM glucagon (n = 3) (I).

(J and K) The mRNA levels of *G6pc* (J) and *Pck1* (K) (n = 3).

(L and M) Male homozygous floxed AMPKα1/2 mice were fed an HFD for 4 weeks, and mice were injected with AAV vectors as described in the STAR Methods. Mice were reated with metformin (50 mg/kg/day) for 3 weeks. Immunoblots of AMPK subunits (L), and a pyruvate tolerance test was conducted (M) (n = 4–5).

(D and L) Each lane represents an individual mouse liver sample. Each bar represents the mean ± SEM. *$p < 0.05$.

KEY RESOURCES TABLE

REAGENT or RESOURCE	SOURCE	IDENTIFIER
Antibodies		
Anti-beta-Actin	Santa Cruz Biotechnology	Cat# sc-81178; RRID:AB_2223230
Anti-CREB	Cell Signaling Technology	Cat# 9197; RRID:AB_331277
Anti-phospho-CREB (Ser133)	Cell Signaling Technology	Cat# 9198, RRID:AB_2561044
Anti-PGC1 alpha	Abcam	Cat# ab72230; RRID:AB_1640773
Anti-phospho-p38 MAPK	Cell Signaling Technology	Cat# 4631; RRID:AB_331765
Anti-p38 MAPK	Cell Signaling Technology	Cat# 8690; RRID:AB_10999090
Anti-Mitofusin-2	Cell Signaling Technology	Cat# 9482; RRID:AB_2716838
Anti-OPA1	Cell Signaling Technology	Cat# 80471; RRID:AB_2734117
Anti-phospho-MFF (Ser146)	Cell Signaling Technology	Cat# 49281; RRID:AB_2799354
Anti-MFF (E5W4M)	Cell Signaling Technology	Cat# 84580; RRID:AB_2728769
Anti-phospho-DRP1 (Ser616)	Cell Signaling Technology	Cat# 4494; RRID:AB_11178659
Anti-phospho-DRP1 (Ser637)	Cell Signaling Technology	Cat# 6319; RRID:AB_10971640
Anti-phospho-AMPK (Thr172)	Cell Signaling Technology	Cat# 2531; RRID:AB_330330
Anti-AMPK-alpha	Cell Signaling Technology	Cat# 2532; RRID:AB_330331
Anti-Mitofusin 1	Abcam	Cat# ab57602; RRID:AB_2142624
Anti-DRP1 (D6C7)	Cell Signaling Technology	Cat# 8570; RRID:AB_10950498
Anti-AMPK alpha 1	Abcam	Cat# ab3759; RRID:AB_304054
Anti-AMPK alpha 2	Abcam	Cat# ab3760; RRID:AB_304055
Anti-AMPK gamma 1	Abcam	Cat# ab32508; RRID:AB_722769
Goat Anti-Rabbit IgG (H L)-HRP Conjugate antibody	Bio-Rad	Cat# 172–1019; RRID:AB_11125143
Goat Anti-Mouse Goat anti-mouse IgG-HRP	Santa Cruz Biotechnology	Cat# sc-2005; RRID:AB_631736
Bacterial and Virus Strains		
AAV8 Virus	Penn Vector Core	AAV8.TBG.PI.Cre.rBG
Chemicals, Peptides, and Recombinant Proteins		
Metformin	Enzo life sciences	Cat# ALX-270–432-G005; CAS Number 1115–70–4
Metformin-^{14}C	Moravek.Inc	Cat# MC-2043
Oligomycin	Sigma Aldrich	Cat# O4876; CAS Number 1404–19–9
Carbonyl cyanide 4-(trifluoromethoxy) phenylhydrazone	Sigma Aldrich	Cat# C2920; CAS Number 370–86–5
Antimycin A	Sigma Aldrich	Cat# A8674; CAS Number 1397–94–0
Rotenone	Sigma Aldrich	Cat# R8875; CAS Number 83–79–4
Sodium pyruvate	Sigma Aldrich	Cat# P8574; CAS Number 113–24–6
Myokinase	Sigma Aldrich	Cat# M3003; CAS Number 9013–02–9
Pyruvate Kinase	Sigma Aldrich	Cat# P1506; CAS Number 9001–59–6
Oil Red O	Sigma Aldrich	Cat# O0625; CAS Number 1320–06–5
Collagen from rat tail	Sigma Aldrich	Cat# C7661; CAS Number 9007–34–5
Adenosine 5′-diphosphate sodium salt	Sigma Aldrich	Cat# A2754; CAS Number 20398–34–9

REAGENT or RESOURCE	SOURCE	IDENTIFIER
Glucagon	Sigma Aldrich	Cat# G2044; CAS Number 16941–32–5
Phosphatase Inhibitor Cocktail 2	Sigma Aldrich	Cat# P5726
Phosphatase Inhibitor Cocktail 3	Sigma Aldrich	Cat# P0044
Phenylmethanesulfonyl fluoride	Sigma Aldrich	Cat# P7626; CAS Number 329–98–6
D-(+)-Glucose	Sigma Aldrich	Cat# G8270; CAS Number 50–99–7
Sodium L-lactate	Sigma Aldrich	Cat# L7022; CAS Number 867–56–1
dCTP, 100mM	promega	Cat# U1221
Phosphoenolpyruvic acid, monopotassium salt	Santa Cruz Biotechnology	Cat# sc-208168; CAS 4265–07–0
Copmplete, Mini	Roche	Cat# 11 836 153 001
Cell Lysis Buffer (10X)	Cell Signaling Technology	Cat# #9803
MitoTracker Red CMXRos	Thermo Fisher Scientific	Cat# M7512
Hoechst 33342	Thermo Fisher Scientific	Cat# H3570; CAS Number 23491–52–3
TRIzol Reagent	Thermo Fisher Scientific	Cat# 15596018
PBS, pH 7.4	Thermo Fisher Scientific	Cat# 10010023
Bovine Serum Albumin Fraction V	Roche	Cat# 3117332001
Protein Assay Dye Reagent Concentrate	Bio-Rad	Cat# 5000006
Alcohol	Fisher scientific	Cat# A995; CAS Number 64–17–5,67–56–1,67–63–0
2-Propanol	Fisher scientific	Cat# A416; CAS Number 67–63–0
Methanol	Fisher scientific	Cat# A412; CAS Number 67–56–1
TBS (Tris buffered saline)	Quality Biological	Cat# 351–086–101
High Salt Precipitation Solution	Molecular Research Center, Inc	Cat# PS 161
BCP Phase Separation Reagent	Molecular Research Center, Inc	Cat# BP151; CAS Number 109–70–6
GlutaMAX	GIBCO	Cat# 35050061
Penicillin-Streptomycin	GIBCO	Cat# 15140122
Sodium Pyruvate (100 mM)	GIBCO	Cat# 11360070
HEPES	GIBCO	Cat# 15630080
Trypsin-EDTA (0.05%), phenol red	GIBCO	Cat# 25300054
Insulin-Transferrin-Selenium (ITS)	Corning	Cat# 25800CR
Insulin	Novolin	Cat# NDC 0169–1834–11
Seahorse XF Palmitate-BSA FAO Substrate	Agilent	Cat# 102720–100
Seahorse XF base medium, without phenol red, 500 mL	Agilent	Cat# 103335–100
William's medium E	GIBCO	Cat# 12551032
DMEM (Dulbecco's Modified Eagle's Medium)	Corning	Cat# 10–014-CV
DMEM (Dulbecco's Modified Eagle's Medium)	Corning	Cat# 10–013-CV
L-glutamine Solution	Corning	Cat# MT25005CI
Fetal Bovine Serum	GIBCO	Cat# 16140071
Critical Commercial Assays		

REAGENT or RESOURCE	SOURCE	IDENTIFIER
Mitochondria Isolation Kit for Cultured Cells (with Dounce Homogenizer) (ab110171)	Abcam	Cat# ab110171
TMRE-Mitochondrial Membrane Potential Assay Kit (ab113852)	Abcam	Cat# ab113852
MitoTox Complex I OXPHOS Activity Assay Kit (ab109903)	Abcam	Cat# ab109903
MitoTox Complex II + III OXPHOS Activity Assay Kit (ab109905)	Abcam	Cat# ab109905
MitoTox Complex IV OXPHOS Activity Assay Kit (ab109906)	Abcam	Cat# ab109906
MitoTox Complex V OXPHOS Activity Assay Kit (ab109907)	Abcam	Cat# ab109907
ATP Determination Kit	Thermo Fisher Scientific	Cat# A22066
Mitochondrial DNA Isolation Kit (ab65321)	Abcam	Cat# ab65321
EnzyChrom Glucose Assay Kit	Bioassay Systems	Cat# EBGL-100
iScript cDNA Synthesis Kit	Bio-Rad	Cat# 1708891
iTaq Universal SYBR® Green Supermix	Bio-Rad	Cat# 1725121
Amersham ECL Prime Western Blotting Detection Reagent	GE Healthcare Life Sciences	Cat# RPN2232
Deposited Data		
DNA Microarray	This paper	GEO: GSE114234
Experimental Models: Cell Lines		
Hepa 1–6	ATCC	CRL-1830
Experimental Models: Organisms/Strains		
Mouse: AMPK α1 floxed	Jackson lab	Stock No. 014141
Mouse: AMPK α2 floxed	Jackson lab	Stock No. 014142
Oligonucleotides		
PKLR 5′-CCAGCAGCATCAGTCGTATATC	This Paper	
PKLR 3′- ACCCAGGAGGAATCGAATTAAC	This Paper	
ND6 5′-GTTTGGGAGATTGGTTGATGTATG	This Paper	
ND6 3′- CACCCAGCTACTACCATCATTC	This Paper	
Software and Algorithms		
Zeisis ZEN 2.6	Zeisi	https://www.zeiss.com/microscopy/us/products/microscope-software/zen.html
Quantity One 1-D Analysis	Bio-rad	https://www.bio-rad.com/en-us/product/quantity-one-1-d-analysis-software?ID=1de9eb3a-1eb5-4edb-82d2-68b91bf360fb
Nis Elements	Nikon	https://www.microscope.healthcare.nikon.com
ImageJ		https://imagej.nih.gov/ij/download.html
Other		
Contour Blood Glucose Monitoring System - Model 9545C	Bayer	Cat# 9545C
Contour blood glucose test strips	Ascensia Diabetes Care US Inc.	Cat# 7097C
NuPAGE 4–12% Bis-Tris Protein Gels, 1.0 mm, 15-well	Thermo Fisher Scientific	Cat# NP0323BOX
NuPAGE 3–8% Tris-Acetate Protein Gels, 1.0 mm, 15-well	Thermo Fisher Scientific	Cat# EA03755BOX

REAGENT or RESOURCE	SOURCE	IDENTIFIER
NuPAGE MOPS SDS Running Buffer	Thermo Fisher Scientific	Cat# NP0001
Seahorse XFe96 FluxPaks	Agilent	Cat# 102416–100
Rodent Diet With 60 kcal% Fat	Research Diets	Cat# D12492